

Preparation of some compounds and study their thermal stability for use in dye sensitized solar cells

Abdulraheem S.A. Almalki ^a, A. Alhadhrami ^a, Rami J. Obaid ^b, Meshari A. Alsharif ^c, Abdel Majid A. Adam ^a, Ivo Grabchev ^d, Moamen S. Refat ^{a,e},

^a Department of Chemistry, Faculty of Science, Taif University, Al-Haweiah, P.O. Box 888, 21974 Taif, Saudi Arabia

^b Department of Chemistry, Faculty of Applied Science, Umm Al-Qura University, Makkah, Saudi Arabia

^c Department of Chemistry, Faculty of Science, University of Tabuk, Tabuk, Saudi Arabia

^d Department "Chemistry and Biochemistry, Physiology and Pathophysiology", Faculty of Medicine, University of Sofia, 1407 Sofia, Bulgaria

^e Department of Chemistry, Faculty of Science, Port Said University, Port Said, Egypt

abstract

The present work aimed to prepare some compounds for use in pigmented solar cells based on charge transfer (CT) complexation. For this purpose, first, several derivatives of 1,8-naphthalimide and benzanthrone fluorescent dyes were synthesized. Secondly, the synthesized fluorescent dyes were complexed with picric acid (PA) acceptor via CT interaction in methanol solvent at room temperature. Then, the synthesized CT complexes were stoichiometrically, spectroscopically and thermally characterized. The results obtained from CHN elemental analyses and spectrophotometric titrations indicated the formation of CT complexes with a molar ratio of 1:1 between the PA and each dye. The spectroscopic and physical parameters (K_{CT} , ϵ_{max} , E_{CT} , f , μ , R_N , I_P , and ΔG°), the band gap energy (E_g), and the kinetic-thermodynamic parameters (E^* , A , ΔS^* , ΔH^* and ΔG^*) were calculated for each CT product in methanol solvent at room temperature. IR results indicated that the complexation between each dye and PA acceptor occurs through $\pi \rightarrow \pi^*$ and proton transfer interactions.

Introduction

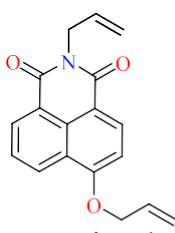
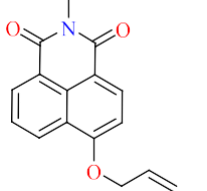
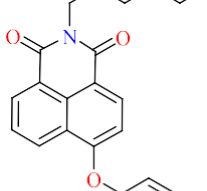
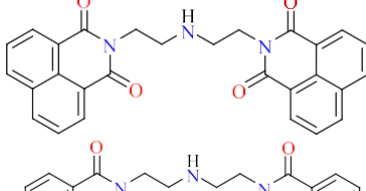
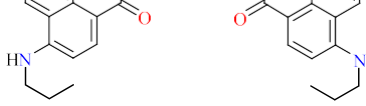
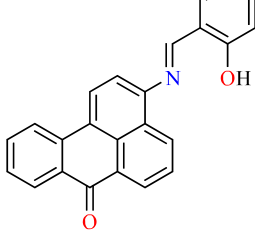
Fluorescent brighteners (FBs) are of interest as prospective polymer modifiers to obtain fluorescent polymers [1]. Among the wide variety of FBs currently used in industry and biomedical research, 1,8-naphthalimide and benzanthrone derivatives have particular interest due to their favorable spectral properties [2–4]. Derivatives of 1,8-naphthalimide benzanthrone dyes exhibit bright colors, strong fluorescence, and high photostability and transport properties, and show wide range of application in chemical and biological research [5]. They are used in: liquid crystals, sensors, polymer brightening, solar energy collectors, daylight fluorescent pigments, membrane studies, in biology as markers and active units, in medicine as antitumor medications, and as dispersing dyes for textile materials [6–20]. Chemical interactions between electron donors (D) and electron acceptors (A) have continued to gain a great deal of attention after more than half a century of sustained research and are one of the most important research topics in many fields of biology, chemistry, medicine, and pharmacology. Such interactions are accompanied with the formation of intensely colored charge transfer (CT) complexes ($D^+ - A^-$) associated by absorption of radiation in the visible or UV regions [21]. CT complexes have a wide range of applications in many fields, like optics, magnetics, electrical conductivity, biochemistry, bioelectrochemical energy transfer processes, and biology [22–31]. Picric acid (PA; $C_6H_3N_3O_7$) is a strong organic acid. The three nitro groups in PA are electron-withdrawing, removing electron density from the aromatic ring and thereby causing it to become a good electron-accepting moiety. The electron-accepting, electron-deficient, and highly acidic nature of PA are responsible for making PA one of the most

commonly-used electron acceptors in CT interactions, as described in many recent studies [32–62].

Our goals in this work were to: (i) synthesize nine derivatives of 1,8-naphthalimide and benzanthrone fluorescent dyes; (ii) synthesize the CT complexes of these fluorescent dyes with PA as the acceptor in methanol solvent at room temperature; (iii) observe the electronic spectral properties of the synthesized CT complexes; (iv) verify the complexation stoichiometry between the dyes and PA acceptor using CHN elemental analysis and spectrophotometric titrations; (v) obtain the spectroscopic data using the Benesi–Hildebrand method; (vi) assess the band gap energy (E_g) of the synthesized CT complexes; (vii) ascertain the mode of interaction between the dyes and PA acceptor using IR spectroscopy; (viii) obtain the thermal properties of the synthesized CT complexes using TG analysis; and (iv) determine the kinetic

Table 1

Chemical structure, chemical formula, molecular weight, and abbreviation of the fluorescent dyes used in this study.

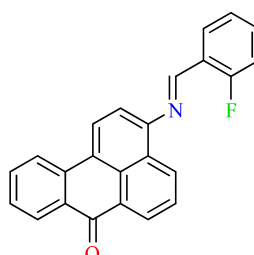
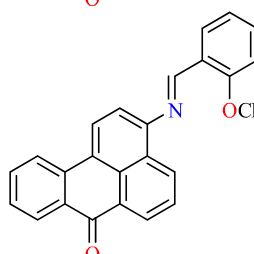
Abbreviation	Chemical structure	Chemical formula	MW (g mol ⁻¹)
Dye 1		C ₁₈ H ₁₇ NO ₃	295
Dye 2		C ₁₉ H ₁₉ NO ₃	309
Dye 3		C ₂₁ H ₂₃ NO ₃	337
Dye 4		C ₂₈ H ₂₁ N ₃ O ₄	463
Dye 5		C ₃₄ H ₃₅ N ₅ O ₄	577
Dye 6		C ₂₄ H ₁₅ NO ₂	349

Dye 7

 $C_{24}H_{14}BrNO$

412

Table 1 (continued)

Abbreviation mol^{-1})	Chemical structure	Chemical formula	MW (g
Day 8		$C_{24}H_{14}BrNO$	412
Dye 9		$C_{25}H_{17}NO_2$	363

thermodynamic data (ΔS^* , ΔH^* , E^* , A , and ΔG^*) using the Coats–Redfern method.

1. Experimental section

1.1. General

All of the reagents and solvents used were of high reagent grade and were obtained from Merck, Fluka or Aldrich Chemical Companies and were directly used for the synthesis with-out further purification. The infrared (IR) spectra (as KBr discs) were collected at room temperature using a Shimadzu FT-IR spectrophotometer over the range of 400–4000 cm^{-1} . The UV–Vis absorption spectra were collected at room temperature using a Genesys 10S UV–Vis spectrophotometer over the range of 320–800 nm with quartz cells (1.0 cm). Elemental per- centage for the elements (%C, %N, and %H) were obtained using a Perkin–Elmer 2400 series CHN microanalyzer. Thermogravimetric (TG) measurements were performed using a Shimadzu TGA–50H ther- mal analyzer with standard platinum TG pans.

1.2. Fluorescent dyes

1.2.1. Synthesis of the dyes

Five 1,8-naphthalimide derivatives (*Dye 1*–*Dye 5*) were synthesized according to methods previously described [63–68]. Four benzanthrone derivatives (*Dye 6*–*Dye 9*) were synthesized according to methods pre- viously described [69–71]. The syntheses were done in a liquid/liquid two-phase system and the products (*Dye 1*–*Dye 9*) were collected in high yield. The synthesized dyes were identified and characterized by their IR and ^1H NMR spectra, elemental analyses, and melting points. Table 1 lists the abbreviation, molecular weight, chemical formula, and chemical structure of the synthesized fluorescent dyes.

1.2.2. Characterization of the synthesized dyes

For the 6-(propoxy)-*N*-allyl-1,8-naphthalimide (*Dye 1*); Yield 82%, m.p. 88–90 °C. FT-IR (KBr) cm^{-1} : 1709 $\nu_{\text{as}}(\text{C}_=\text{O})$, 1660 $\nu_{\text{a}}(\text{C}_=\text{O})$, 1533 $\nu(\text{C}_-\text{C})$, 1152 $\nu_{\text{as}}(\text{C}\text{=}\text{N})$, 1093 $\nu_{\text{s}}(\text{C}\text{=}\text{N})$. ^1H NMR (600 MHz, DMSO d_6): δ = 0.90 (t, 3H, $\text{OCH}_2\text{CH}_2\text{CH}_3$), 1.74 (m, 2H, OCH_2CH_2), 4.06 (t, 2H, OCH_2), 4.93 (d, 2H, NCH_2), 5.22 (m, 2H, $-\text{CH}_2$); 5.87 (m, 1H, $-\text{CH}_-$); 6.89–8.45 (m, 5H, ArH). Analysis: $\text{C}_{18}\text{H}_{17}\text{NO}_3$ (295 g mol $^{-1}$); Calc. (%): C 73.23, H 5.77, N 4.74. Found (%): C 73.27, H 5.86, N 4.70. For the 6-(allyloxy)-*N*-butyl-1,8-naphthalimide (*Dye 2*); Yield 85%, m.p. 82–84 °C. FT-IR (KBr) cm^{-1} : 1701 $\nu_{\text{as}}(\text{C}_=\text{O})$, 1652 $\nu_{\text{a}}(\text{C}_=\text{O})$, 1536 $\nu(\text{C}_-\text{C})$, 1155 $\nu_{\text{as}}(\text{C}\text{=}\text{N})$, 1096 $\nu_{\text{s}}(\text{C}\text{=}\text{N})$. ^1H NMR (600 MHz, DMSO d_6): δ = 0.98 (t, 3H, CH_3); 1.54 (m, 4H, 2 \times CH_2); 3.26 (t, 2H, NCH_2); 4.56 (m, 2H, OCH_2); 5.20 (m, 2H, $-\text{CH}_2$); 5.82 (m, 1H, $-\text{CH}_-$); 7.60–6.68 (m, 2H, ArH); 8.56–7.94 (m, 3H, ArH). Analysis: $\text{C}_{19}\text{H}_{19}\text{NO}_3$ (309 g mol $^{-1}$); Calc. (%): C 73.78, H 6.14, N 4.54. Found (%): C 74.45, H 6.23, N 4.46.

For the 6-(allyloxy)-*N*-hexyl-1,8-naphthalimide (*Dye 3*); Yield 86%, m.p. 63–65 °C. FT-IR (KBr) cm^{-1} : 1705 $\nu_{\text{as}}(\text{C}_=\text{O})$, 1634 $\nu_{\text{a}}(\text{C}_=\text{O})$, 1534 $\nu(\text{C}_-\text{C})$, 1152 $\nu_{\text{as}}(\text{C}\text{=}\text{N})$, 1092 $\nu_{\text{s}}(\text{C}\text{=}\text{N})$. ^1H NMR (600 MHz, DMSO d_6): δ = 0.96 (t, 3H, CH_3); 1.48 (m, 8H, 4 \times CH_2); 3.22 (t, 2H, NCH_2); 4.52 (m, 2H, OCH_2); 5.24 (m, 2H, $-\text{CH}_2$); 5.84 (m, 1H, $-\text{CH}_-$); 7.58–6.72 (m, 2H, ArH); 8.52–7.98 (m, 3H, ArH). Analysis: $\text{C}_{21}\text{H}_{23}\text{NO}_3$ (337 g mol $^{-1}$); Calc. (%): C 74.77, H 6.83, N 4.16. Found (%): C 74.01, H 6.74, N 4.21.

For the *N,N'*-[iminobis(ethane-2,1-diyl)]bis(1,8-naphthalimide) (*Dye 4*); Yield 80%, m.p. 179–181 °C. FT-IR (KBr) cm^{-1} : 3207 $\nu(\text{N}\text{=}\text{N}\text{H})$, 1709 $\nu_{\text{as}}(\text{C}_=\text{O})$, 1659 $\nu_{\text{a}}(\text{C}_=\text{O})$, 1598 $\delta(\text{N}\text{=}\text{N}\text{H})$, 1540 $\nu(\text{C}_-\text{C})$, 1159 $\nu_{\text{as}}(\text{C}\text{=}\text{N})$, 1088 $\nu_{\text{s}}(\text{C}\text{=}\text{N})$. ^1H NMR (600 MHz, DMSO d_6): δ = 3.02 (t, 4H, 2 CH_2 , $\text{NH}-\text{CH}_2$), 3.65 (t, 4H, 2 CH_2 , $\text{CON}-\text{CH}_2$), 4.05 (s, 1H, NH), 7.79–8.41 (m, 12H, aromatic). Analysis: $\text{C}_{28}\text{H}_{21}\text{N}_3\text{O}_4$ (463 g mol $^{-1}$); Calc. (%): C 72.55, H 4.56, N 9.06. Found (%): C 72.62, H 4.65, N 9.00.

For the *N,N'*-[iminobis(ethane-2,1-diyl)]bis((6-(*N*-propylamino))-1,8-naphthalimide) (*Dye 5*); Yield 79%, m.p. 193–195 °C. FT-IR (KBr)

cm^{-1} : 3130 $\nu(\text{N}-\text{H})$, 1702 $\nu_{\text{as}}(\text{C=O})$, 1641 $\nu_{\text{a}}(\text{C=O})$, 1603 $\delta(\text{N}-\text{H})$, 1541 $\nu(\text{C=C})$, 1149 $\nu_{\text{as}}(\text{C}\equiv\text{N})$, 1089 $\nu_s(\text{C}\equiv\text{N})$. ^1H NMR (600 MHz,

DMSO d_6): $\delta = 0.95$ (t, 6H, 2CH₃, CH₃CH₂CH₂NH), 1.58 (m, 4H, 2CH₂, CH₃CH₂CH₂NH), 3.06 (t, 4H, 2CH₂, NH-CH₂-CH₂NCO), 3.12 (t, 4H, 2CH₂, CH₃CH₂CH₂NH), 3.44 (t, 2H, 2CH₂, NH-CH₂-CH₂NCO), 4.04 (s, 1H, NH

aliphatic), 6.86 (s, 1H, NH Aromatic), 7.82–8.47 (m, 10H, aromatic). Analysis: C₃₄H₃₅N₅O₄ (577 g mol⁻¹); Calc. (%): C 70.70, H 6.10, N 12.13. Found (%): C 70.60, H 6.07, N 12.20.

For the 3-(2-hydroxybenzylideneamino)-7H-benzo[*de*]anthracen-7-one (*Dye 6*); Yield 83%, m.p. 170–172 °C. FT-IR (KBr) cm^{-1} : 1634

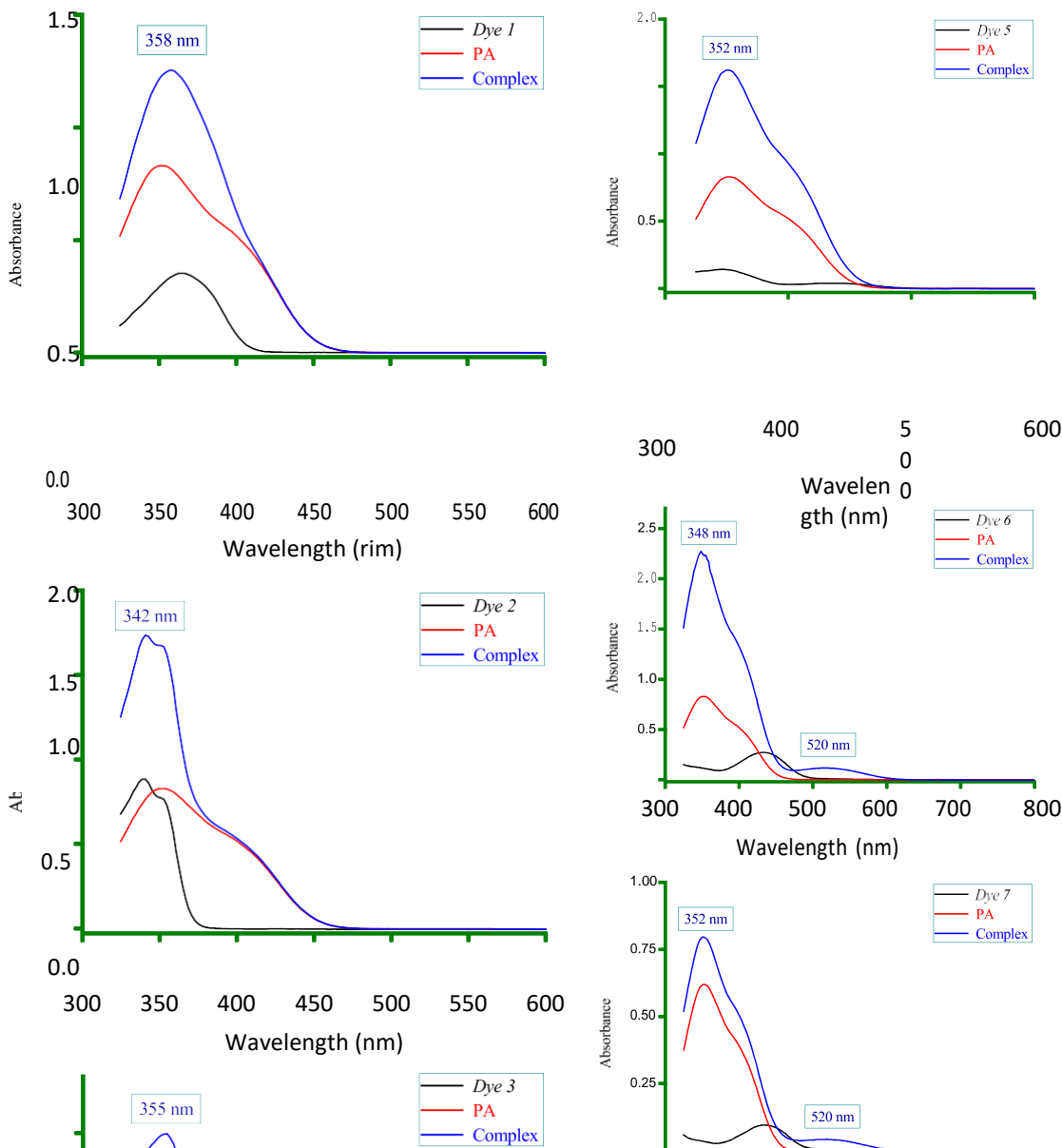
$\nu(\text{C=O})$, 1604 $\nu(\text{C-N})$, 1534 $\nu(\text{C-C})$, 1261 $\delta(\text{C}\equiv\text{C})$. ^1H NMR

(600 MHz, DMSO d_6): $\delta = 6.78$ –8.42 (m, 14H, aromatic); 12.03 (s, 1H, OH). Analysis: C₂₄H₁₅NO₂ (349 g mol⁻¹); Calc. (%): C 82.51, H 4.31, N 4.02. Found (%): C 82.44, H 4.35, N 3.96.

For the 3-(2-bromobenzylideneamino)-7H-benzo[*de*]anthracen-7-one (*Dye 7*); Yield 85%, m.p. 176–178 °C. FT-IR (KBr) cm^{-1} : 1643

$\nu(\text{C=O})$, 1603 $\nu(\text{C-N})$, 1532 $\nu(\text{C-C})$, 1268 $\delta(\text{C}\equiv\text{C})$. ^1H NMR

(600 MHz, DMSO d_6): $\delta = 6.96$ –8.33 (m, 14H, aromatic). Analysis:



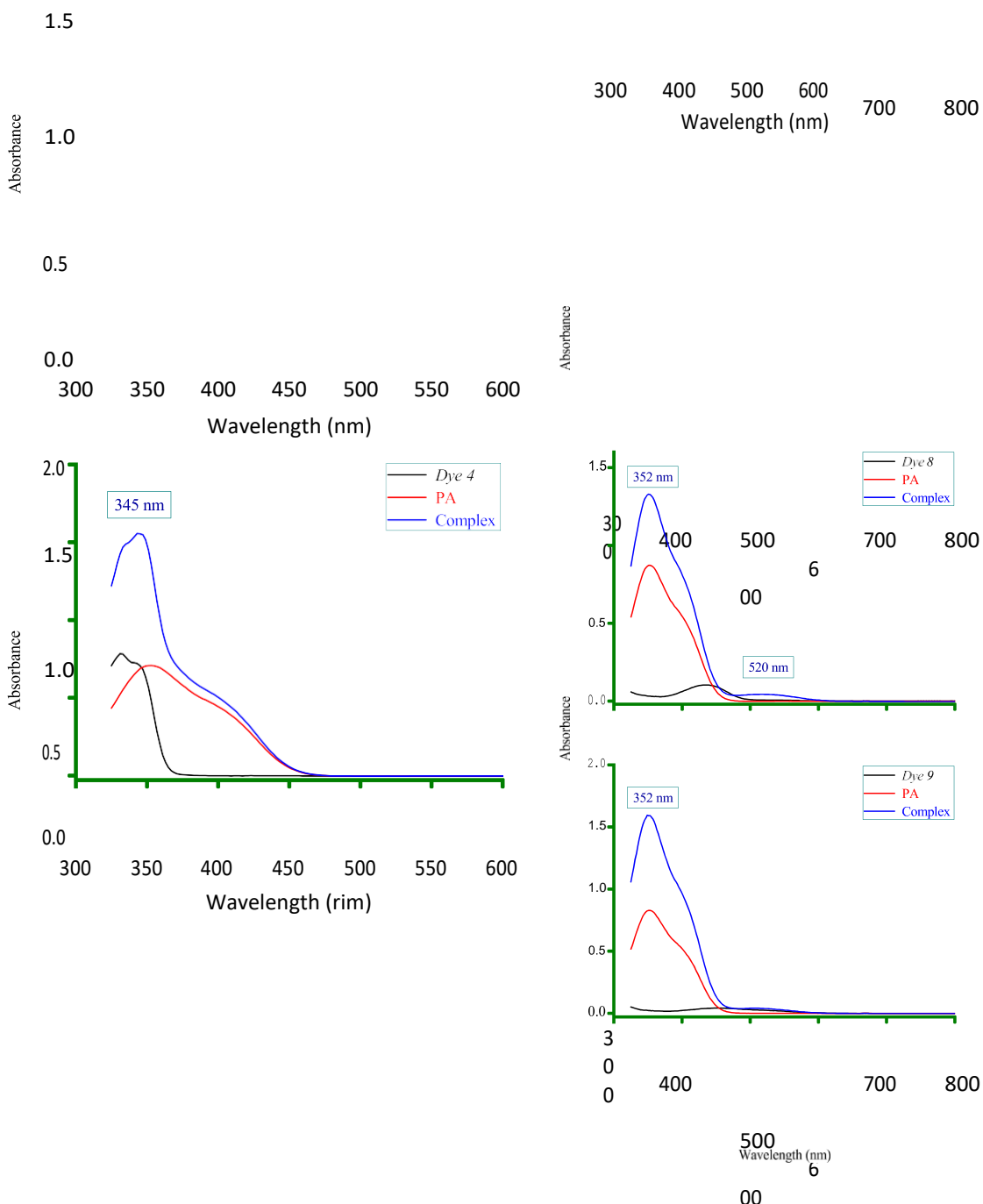


Fig. 1. Electronic absorption spectra of the synthesized CT complexes in methanol solvent at room temperature.

Table 2

Microanalytical data of the synthesized CT complexes.

CT complex	Molecular formula Elemental analyses		Mwt. g mol ⁻¹	Molar ratio					
				C%		H%		N%	
				Found	Cal	Found	Calc.	Found	Calc.
Dye 1-PA	C ₂₄ H ₂₀ N ₄ O ₁₀	524	54.91	54. 96	3.78	3.82	10.75	10.69	1: 1
Dye 2-PA	C ₂₅ H ₂₂ N ₄ O ₁₀	538	55.70	55. 76	4.18	4.09	10.36	10.41	1: 1
Dye 3-PA	C ₂₇ H ₂₆ N ₄ O ₁₀	566	57.17	57. 24	4.52	4.59	9.95	9.89	1: 1
Dye 4-PA	C ₃₄ H ₂₄ N ₆ O ₁₁	692	59.03	58. 96	3.42	3.47	12.22	12.14	1: 1
Dye 5-PA	C ₄₀ H ₃₈ N ₈ O ₁₁	806	59.64	59. 55	4.77	4.71	13.83	13.90	1: 1
Dye 6-PA	C ₃₀ H ₁₈ N ₄ O ₉	578	62.24	62. 28	3.15	3.11	9.60	9.69	1: 1
Dye 7-PA	C ₃₀ H ₁₇ BrN ₄ O ₈	641	56.25	56. 16	2.73	2.65	8.82	8.74	1: 1
Dye 8-PA	C ₃₀ H ₁₇ FN ₄ O ₈	580	62.15	62. 07	2.88	2.93	9.57	9.66	1: 1
Dye 9-PA	C ₃₁ H ₂₀ N ₄ O ₉	592	62.77	62. 84	3.29	3.38	9.50	9.46	1: 1

C₂₄H₁₄BrNO (412 g mol⁻¹); Calc. (%): C 69.89, H 3.39, N 3.41. Found (%): C 69.96, H 3.46, N 3.47.

For the 3-(2-fluorobenzylideneamino)-7H-benzo[de]anthracen-7-one (Dye 8); Yield 80%, m.p. 171–173 °C. FT-IR (KBr) cm⁻¹: 1639 ν(C=O), 1608 ν(C=N), 1528 ν(C=C), 1262 δ(C≡C). (600 MHz, DMSO *d*₆): δ = 7.12–8.23 (*m*, 14H, aromatic). Analysis: C₂₄H₁₄FNO (351 g mol⁻¹); Calc. (%): C 82.06, H 4.01, N 4.02. Found (%): C 82.01, H 4.08, N 3.95.

For the 3-(2-methoxybenzylideneamino)-7H-benzo[de]anthracen-7-one (Dye 9); Yield 84%, m.p. 172–174 °C. FT-IR (KBr) cm⁻¹: 1636 ν(C=O), 1606 ν(C=N), 1526 ν(C=C), 1272 δ(C≡C). (600 MHz, DMSO *d*₆): δ = 3.72 (*s*, 3H, CH₃), 6.69–8.36 (*m*, 14H, aromatic). Analysis: C₂₅H₁₇NO₂ (363 g mol⁻¹); Calc. (%): C 82.66, H 4.69, N 3.87. Found (%): C 82.58, H 4.60, N 3.96.

1.3. CT complexes

1.3.1. Synthesis of the CT complexes

An methanolic solution containing 1 mmol of each dye was mixed with an methanolic solution of PA acceptor (1 mmol) and stirred for ca. 30 min at room temperature on a magnetic stirrer. The mixture was reduced to one-half by evaporation on a water bath. All the solid CT products were prepared by the same method. The CT products were filtered off and washed with methanol. Finally, the

products were collected and dried in vacuo for 48 h [72–75].

1.3.2. Stoichiometry determination

1.3.2.1. *In solid-state*. To obtain the stoichiometry of the Dye-PA interaction in solid form and to realize the purity and the constituents of the obtained complex, microanalytical analysis of the C, N and H contents were determined using a Perkin-Elmer 2400 series CHN microanalyzer.

1.3.2.2. *In liquid-state*. The stoichiometry of the Dye-PA interaction in the liquid-state in methanol solvent was acquired by the determination of the conventional molar ratio using the spectrophotometric titrations

at room temperature. A 4.0, 3.5, 3.0, 2.5, 2.0, 1.5, 1.0, 0.75, 0.5, or 0.25 mL of 5.0 × 10⁻⁴ M PA standard solution in the appropriate solvent was added to 1.00 mL of 5.0 × 10⁻⁴ M dye solution. The concentration of the PA acceptor (C_a) was varied from 4.00 × 10⁻⁴ M to 0.25 × 10⁻⁴ M whereas the concentration of the dye (C_dC°) was kept at

and the electronic spectrum of each Dye–PA reaction was then collected against a reagent blank solution. Fig. 1 shows the electronic spectra of the synthesized dyes (5.0×10^{-4} M), the PA acceptor (5.0×10^{-4} M) and the resulting CT complexes in methanol in the region of

320–800 nm. The PA acceptor has a strong absorption yellow color. It displays a strong broad absorption band from 300 nm to 450 nm with a maximum at 351 nm.

Solution of Dye 1, Dye 2, Dye 3, and Dye 4 at a 5.0×10^{-4} M in methanol solvent display a strong broad absorption

band with a maximum at 365, 339, 355, and 332 nm, respectively. Solution of Dye 6, Dye 7, and Dye 8 at a 5.0×10^{-4} M in methanol solvent display a medium absorption band with a maximum at 433, 436, and

436 nm, respectively. Dye 5 and Dye 9 show a weak broad long-wave band around 300–550 nm. The spectrum of Dye 5 has a λ_{max} at 345 nm, while that of the Dye 9 is 352 nm. With the addition of PA to each dye solution, an intense, very strong, broad band was observed in the visible region. Spectra of CT complexes formed with Dye 1, Dye 2, Dye 3, Dye 4, and Dye 6 display absorption maxima at 358, 342, 355, 345, and 348 nm, respectively. The CT complexes of Dye 5, Dye 7, Dye 8, and Dye 9 exhibit maximum absorption band at 352 nm. These strong broad bands are indicative of the formation of the H-bonded

5.0×10^{-4} M, to obtain solutions with a (Dye: PA) molar ratio that var-

ied from 1:4 to 4:1. The absorbance of each CT complex was measured and plotted against the volume of the added PA acceptor.

2. Results and discussion

2.1. Electronic spectra

The PA acceptor (5.0×10^{-4} M) was mixed with each synthesized dye solution (5.0×10^{-4} M) in methanol solvent at room temperature,

complex between the dye and PA. A new absorption band appear in the spectrum of the Dye 6–PA, Dye 7–PA, and Dye 8–PA complex at λ_{max} 520 nm, while the free dyes and PA display no measurable absorption band at that wavelength.

3.2. Stoichiometry of the CT interaction

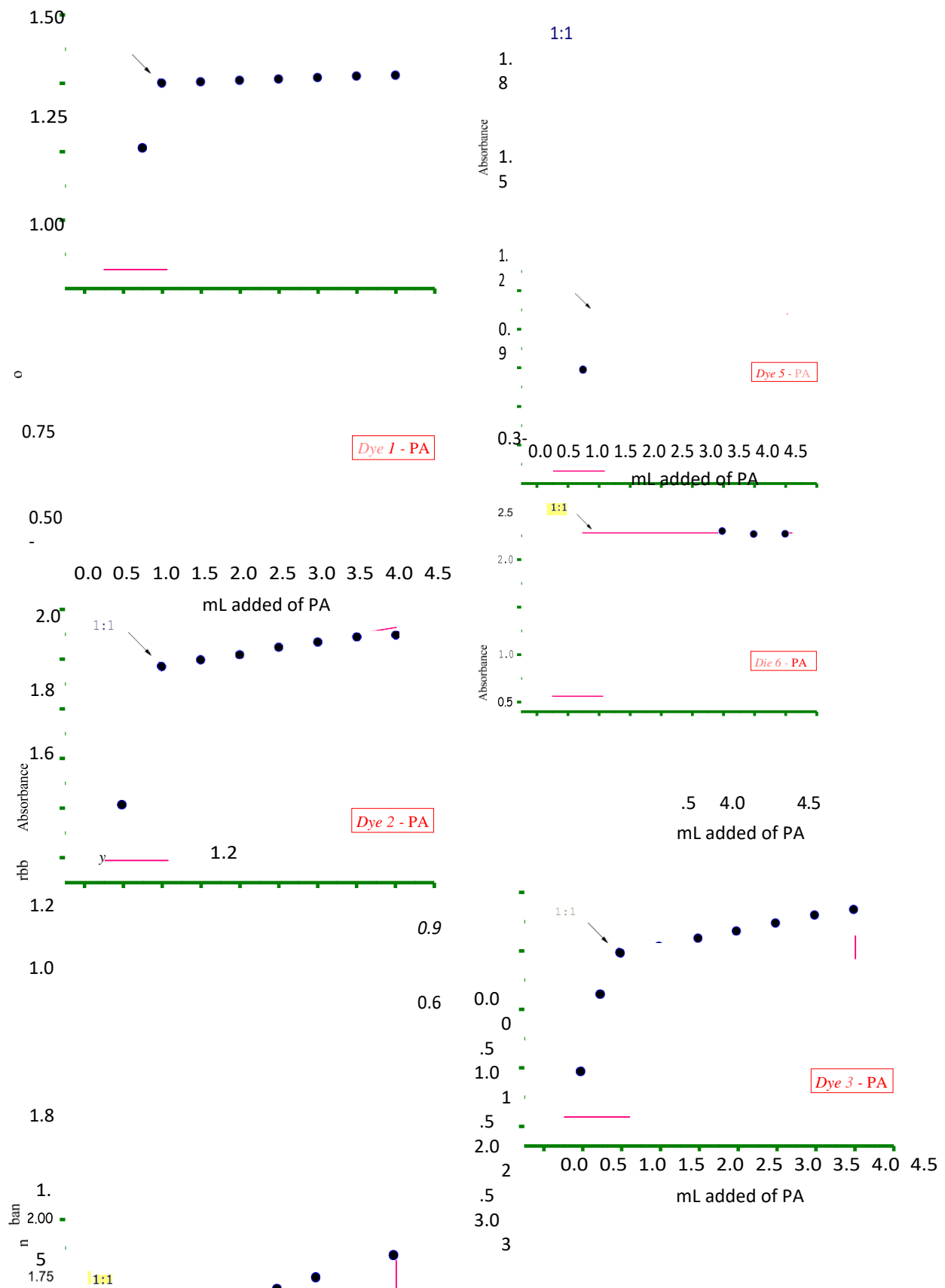
The stoichiometry of the CT interaction between PA acceptor and each dye in solid form was obtained to realize the purity and the constituents of the CT products. The results of the elemental analyses of these CT products were listed in Table 2. The calculated values are in good agreement with the experimental values of carbon, hydrogen, and nitrogen which indicate that the obtained CT products were free of impurities. The stoichiometry of the CT interaction between the dyes and the PA acceptor was found to be 1:1. The stoichiometry of the CT interactions in solution was determined using the spectrophotometric titration method. The electronic spectrum of each CT interaction was obtained at varying PA acceptor concentration and a constant dye concentration in methanol solvent at room temperature. The stoichiometry of each CT interaction was obtained graphically by plotting the volume of PA accep-

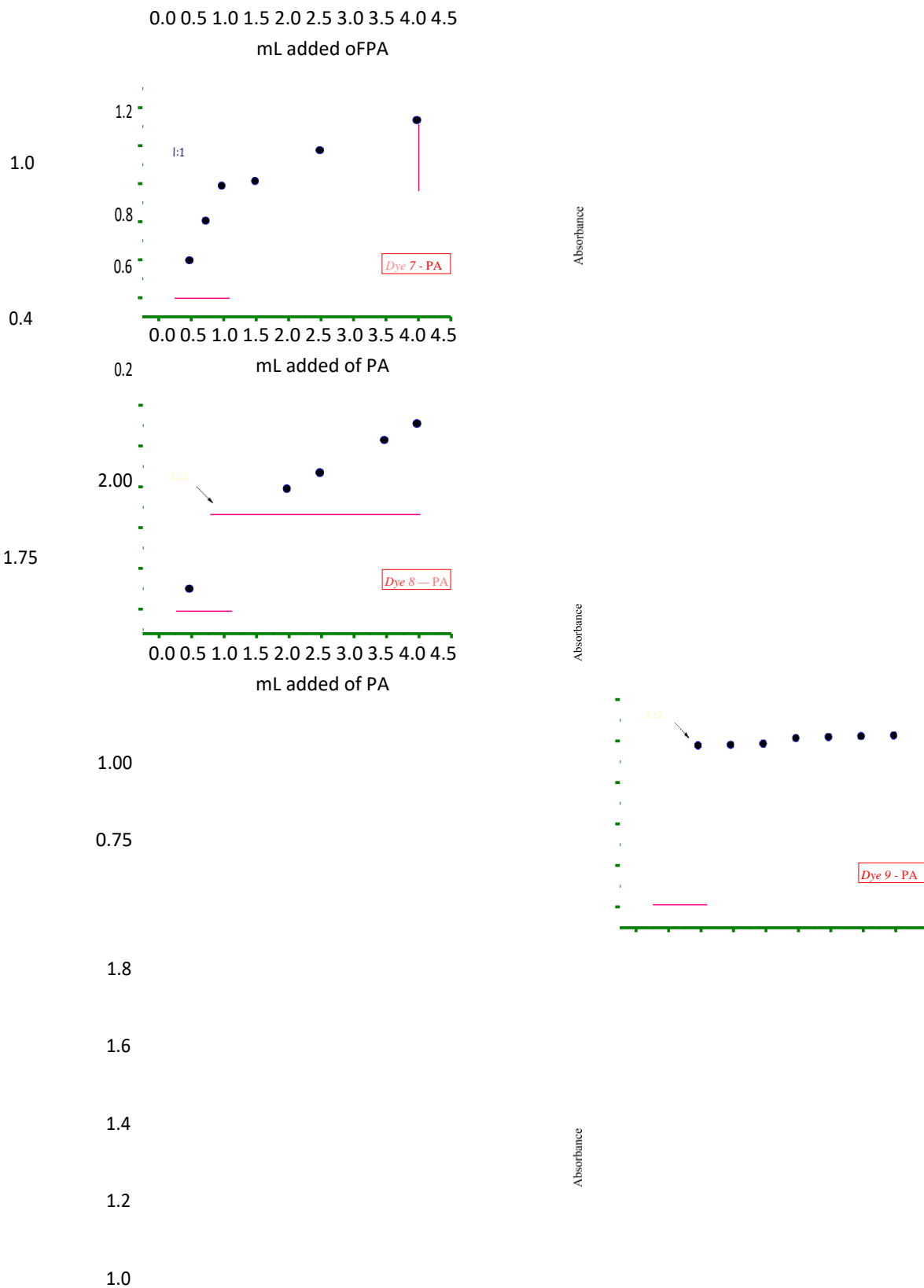
tor against the absorbance as shown in Fig. 2. The plots in this figure indicate that the greatest interaction between each dye and PA occurred

at a Dye: PA ratio of 1:1.

3.3. Spectroscopic parameters

The spectroscopic parameters such as the molar extinction coefficient, ϵ_{max} ($\text{L mol}^{-1} \text{cm}^{-1}$); the formation constant, K_{CT} (L mol^{-1}); the energy of interaction, E_{CT} (eV); the standard free energy, ΔG° (kJ mol^{-1}); the transition dipole moment, μ ; the oscillator strength, f ;





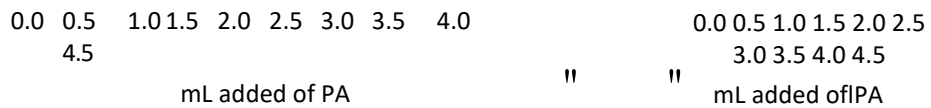
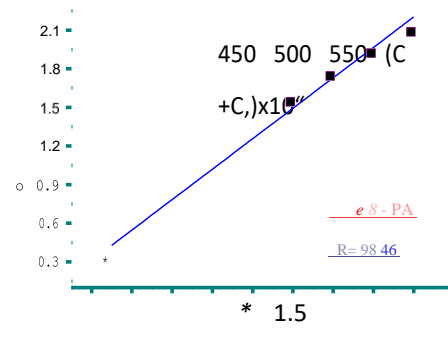
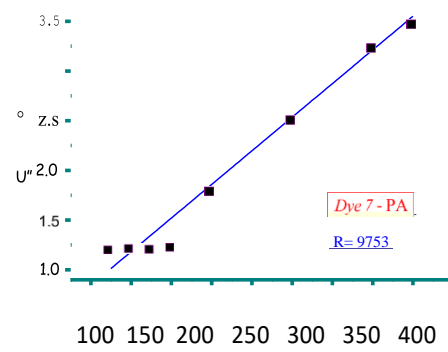
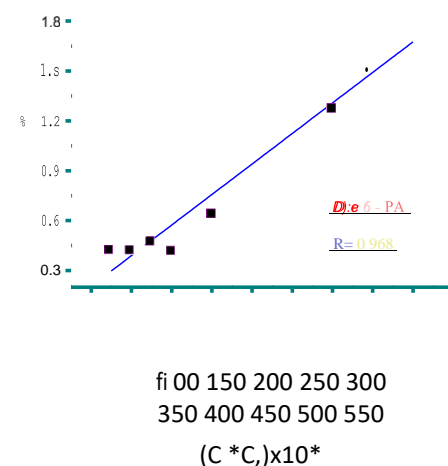
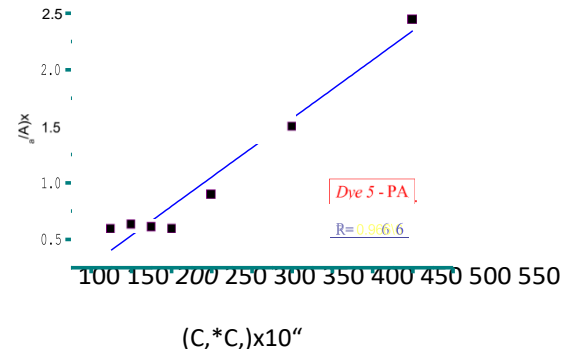
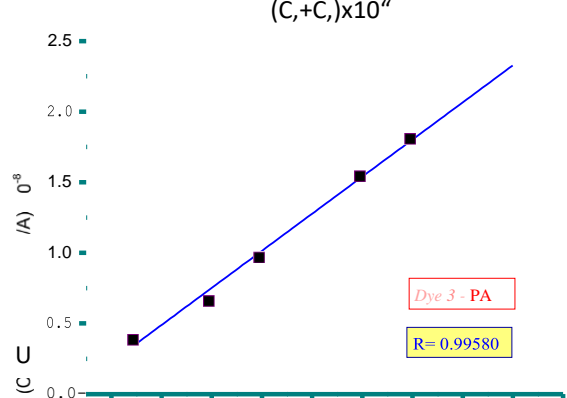
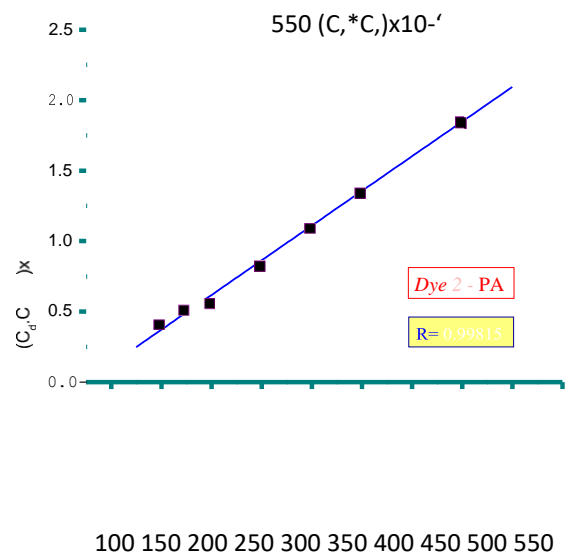
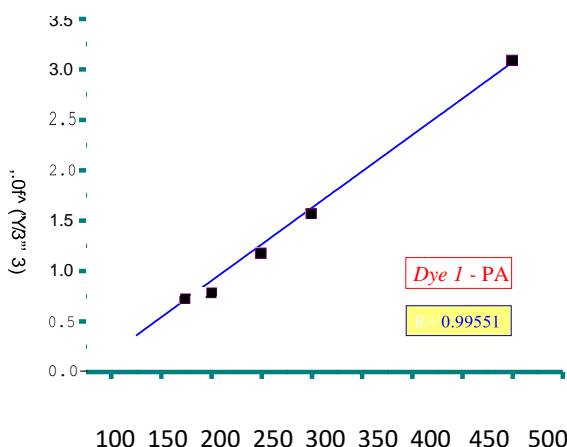


Fig. 2. Spectrophotometric titration curves for the synthesized CT complexes in methanol solvent at room temperature.



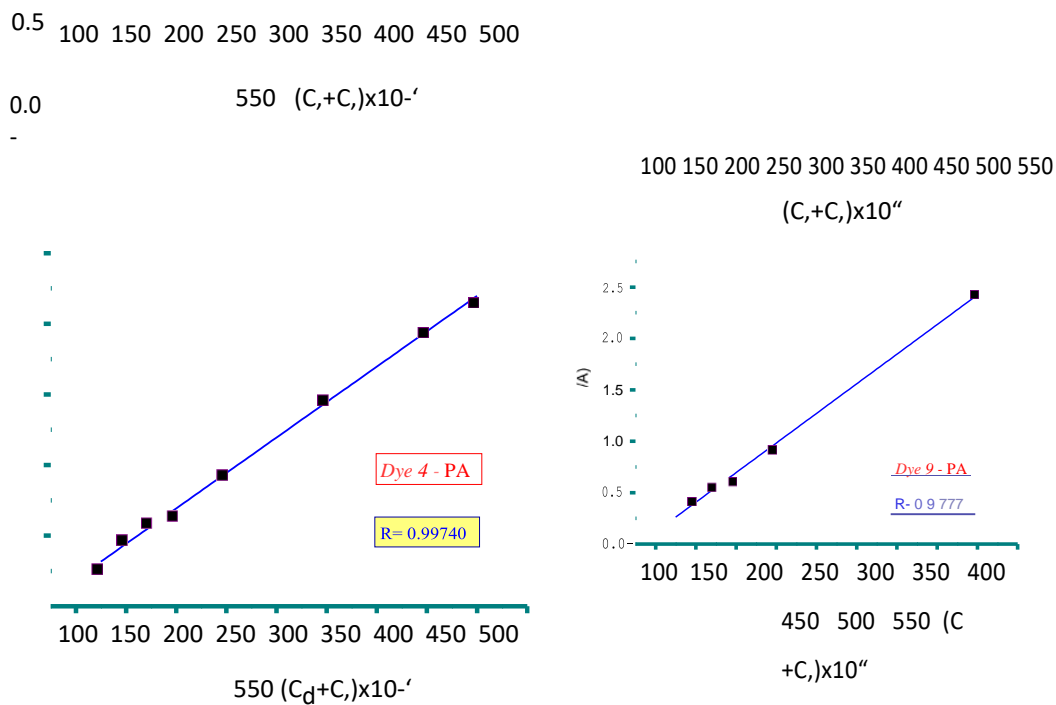


Fig. 3. The 1:1 Benesi–Hildebrand plots for the synthesized CT complexes in methanol solvent at room temperature.

Table 3

Spectroscopic and physical data of the synthesized CT complexes at room temperature.

Complex	λ_{max} (nm)	E_{CT} (eV)	K ($Lmol^{-1}$)	ϵ_{max} ($Lmol^{-1} cm^{-1}$)	f	μ	I_p	R_N	ΔG° (kJ mol $^{-1}$)
Dye 1-PA	358	3.47	1.33×10^5	14×10^5	0.60	2.13	10.0	0.977	-34,944
Dye 2-PA	342	3.63	1.33×10^5	20×10^5	1.46	3.26	10.2	1.030	-34,952
Dye 3-PA	355	3.50	1.74×10^5	19×10^5	0.82	2.49	10.0	0.989	-35,613
Dye 4-PA	345	3.60	1.61×10^5	20×10^5	1.43	3.24	10.2	1.020	-35,408
Dye 5-PA	352	3.53	2.13×10^5	19×10^5	0.83	2.49	10.1	0.998	-36,114
Dye 6-PA	348	3.57	2.25×10^5	27×10^5	1.18	2.95	10.2	10.10	-36,250
Dye 7-PA	352	3.53	4.09×10^5	14×10^5	0.64	2.18	10.1	0.995	-37,726
Dye 8-PA	352	3.53	2.90×10^5	21×10^5	0.91	2.61	10.1	0.999	-36,872
Dye 9-PA	352	3.53	1.26×10^6	17×10^5	0.75	2.37	10.1	0.997	-34,802

the ionization potential, I_p (eV); and the resonance energy, R_N ; were calculated for each CT complex as follows:

3.3.1. Calculation of ϵ_{max} and K_{CT}

Both the ϵ_{max} and K_{CT} value were calculated based on the 1:1 Benesi–Hildebrand equation [76]:

$$\frac{1}{\epsilon_{CT}} = \frac{1}{K_{CT}} + \frac{1}{\epsilon_0} \cdot \frac{C_d}{C_a} \quad (1)$$

where A is the absorbance of the detected CT^a band, C_a and C_d are the initial concentrations of the PA and the dye, respectively. A straight line was obtained when plotting the $(C_a C_d)/A$ values against the corresponding $(C_a + C_d)(C_a + C_d)$ values. The intercept and the slope of this line equal $1/K_{CT}$ and $1/\epsilon_0$, respectively.

3.3.2. Calculation of E_{CT}

The E_{CT} value was calculated based on the equation derived by Briegleb [77]:

$$E_{CT} = \frac{\lambda_{CT} \cdot \log K_{CT}}{\lambda_{CT} - \lambda_{max}} \quad (2)$$

where λ_{CT} and λ_{max} are the wavelength of the CT complex and the maximum absorption wavelength of the dye, respectively.

3.3.4. Calculation of μ

The value of μ was calculated using Eq. (4) [79]:

$$\mu = 0.0958 \cdot \epsilon_{max} \cdot v_{max}^{1/2} \quad (4)$$

3.3.5. Calculation of f

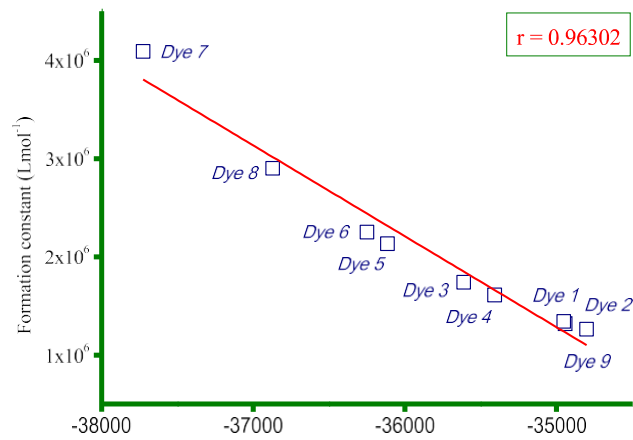
The f can be derived from the absorption spectrum using an approximate formula (Eq. (5)) [80]:

3.3.3. Calculation of ΔG°

The ΔG° value was calculated from the formation constant using Eq. (3) [78].

T is the absolute temperature in Kelvin, and R is equal to $8.314 \text{ J mol}^{-1} \text{ K}^{-1}$ (gas constant).

$$\Delta G^\circ = -2.303RT \log K_{CT} \quad (3)$$



$$f \approx 4:319 \times 10^{-9} \int_{\infty}^{\infty} \epsilon_{max} dv$$

05

p

The $\int \epsilon_{max} dv$ is the area under the curve of the ϵ_{max} of the absorption band. For an initial approximation, f can be calculated using Eq. (6):

$$f \approx 4:319 \times 10^{-9} \epsilon_{max} v_{1/2}$$

06

where $v_{1/2}$ is the full width at half the maximum in cm^{-1} .

3.3.6. Calculation of I_p

Ionization potential (I_p) is the energy required to remove an electron from the highest occupied molecular orbital. It's used to measure the electron-donating power of a dye molecule. The I_p value was calculated using Eq. (7) [81]:

$$I_p \delta eV \approx 5:76 \times 1:53 \times 10^{-4} v_{CT}$$

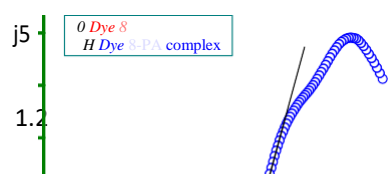
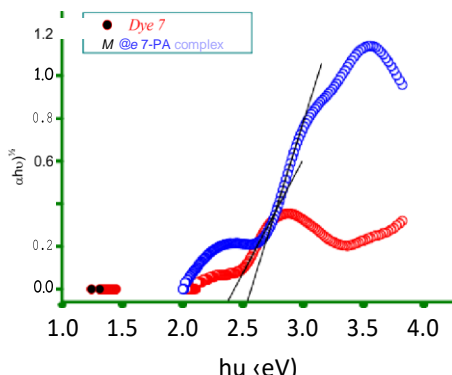
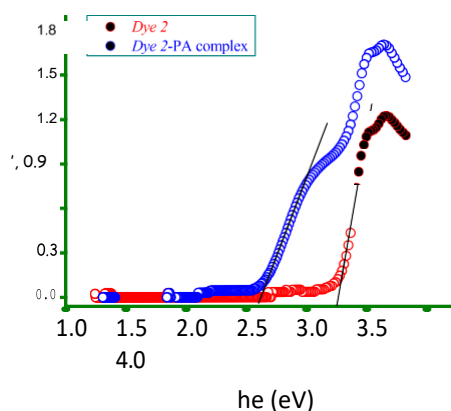
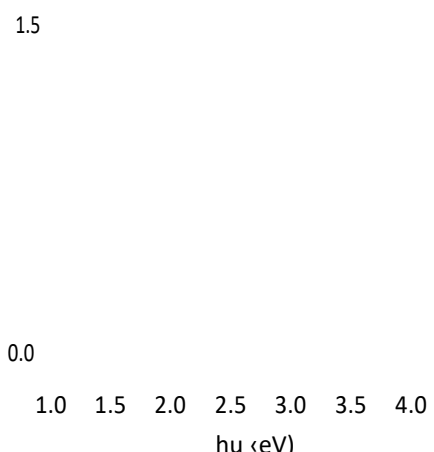
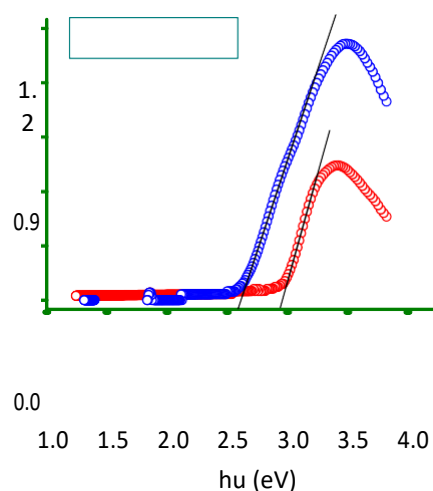
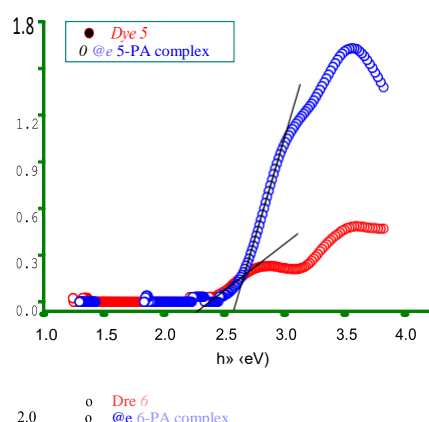
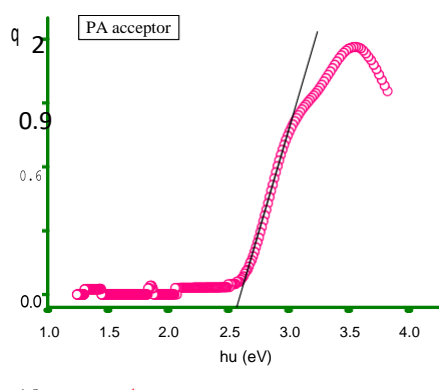
07p

Dye-PA complex

Fig. 4. Values of the formation constant (K_{CT}) for the synthesized CT complexes.

Standard free energy (kJ mol^{-1})

Fig. 5. Linear correlations between the standard free energy (ΔG°) and the formation constant (K_{CT}) for the synthesized complexes.



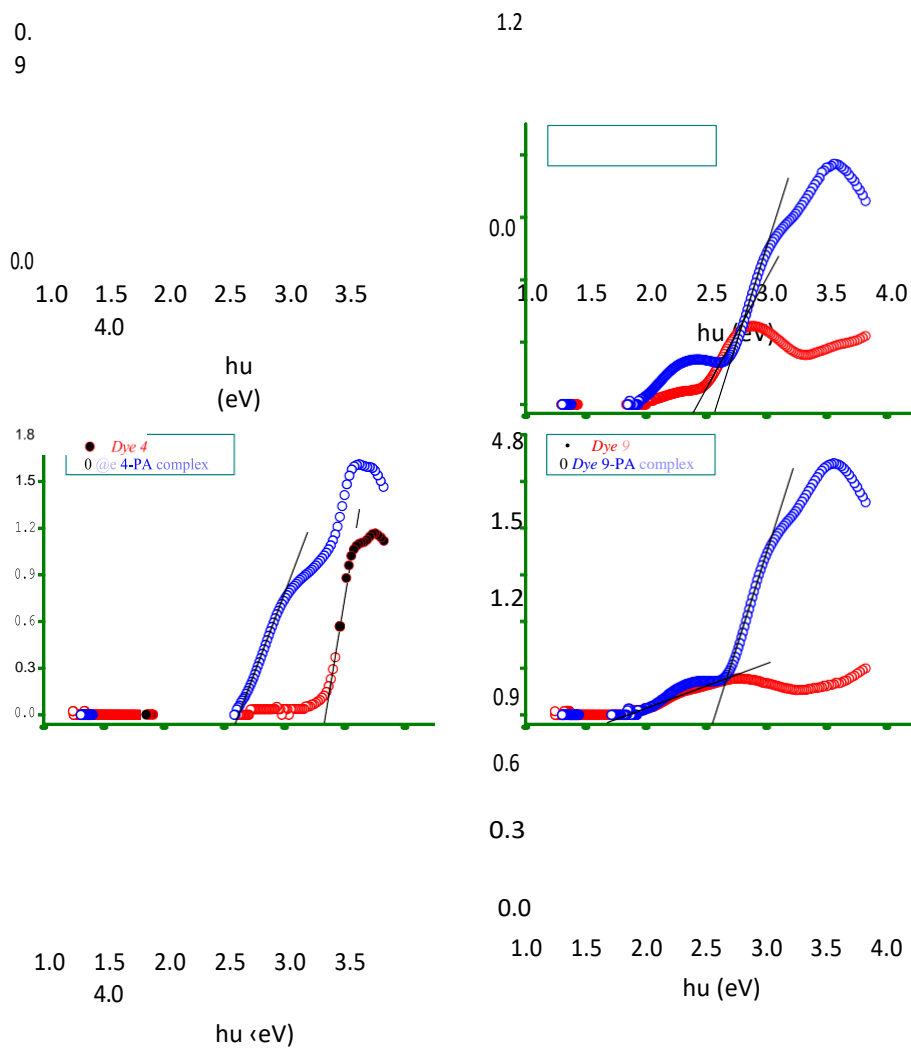


Fig. 6. Plots of $(\alpha h\nu)^{1/2}$ against $h\nu$ for the PA acceptor, free dyes, and the synthesized CT complexes.

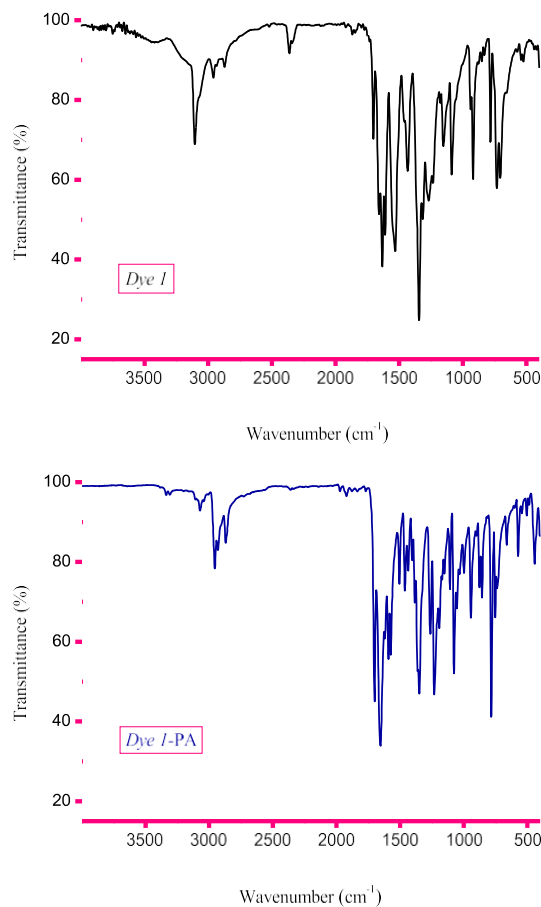


Fig. 7. IR spectra of the free *Dye 1* and its CT complex with PA acceptor.

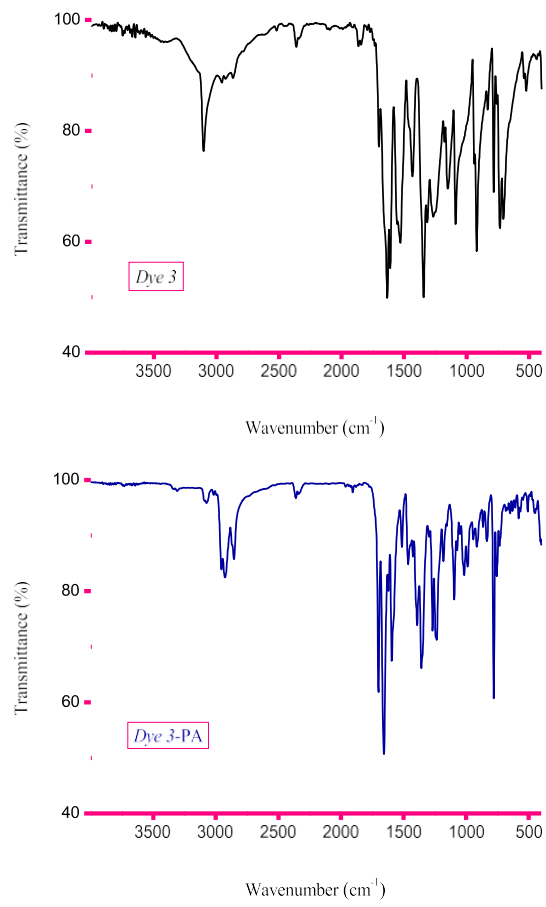
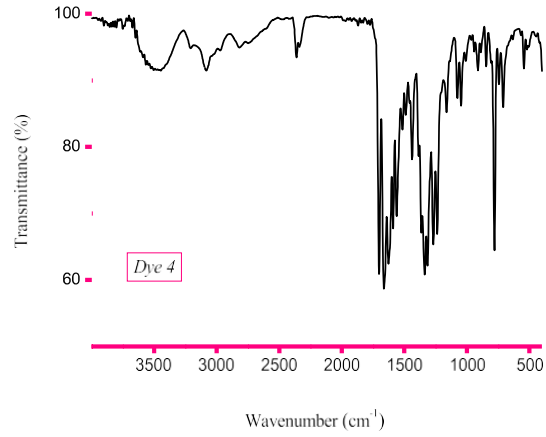
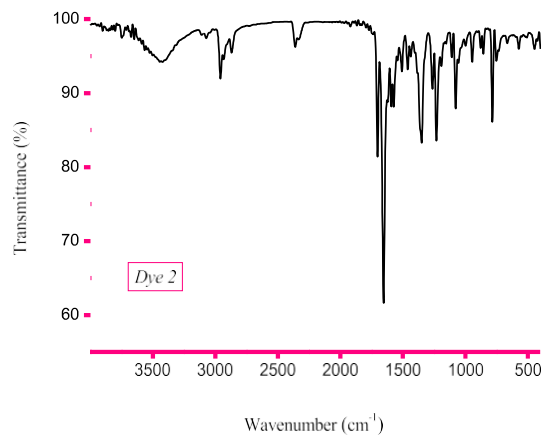


Fig. 9. IR spectra of the free *Dye 3* and its CT complex with PA acceptor.



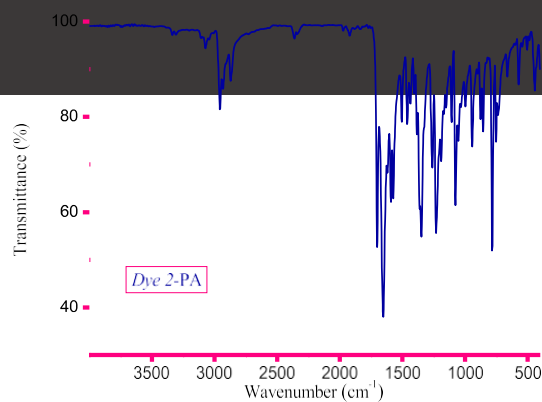


Fig. 8. IR spectra of the free Dye 2 and its CT complex with PA acceptor.

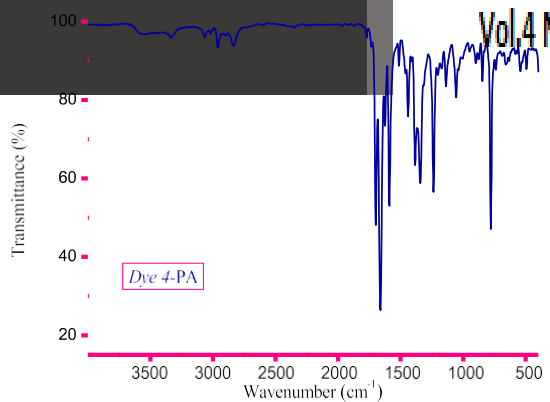


Fig. 10. IR spectra of the free Dye 4 and its CT complex with PA acceptor.

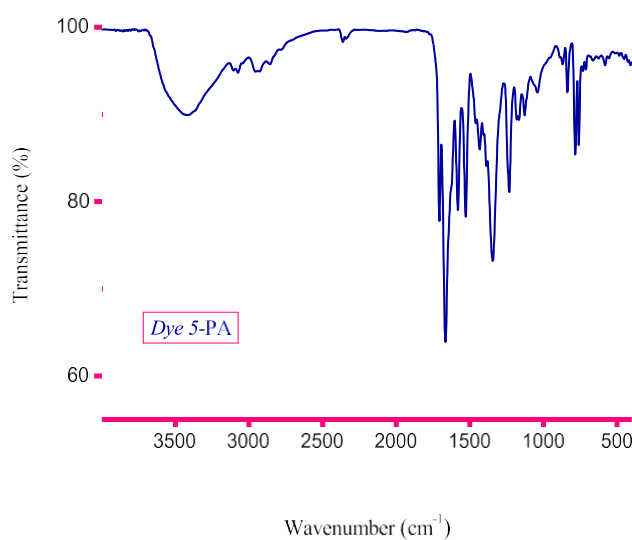
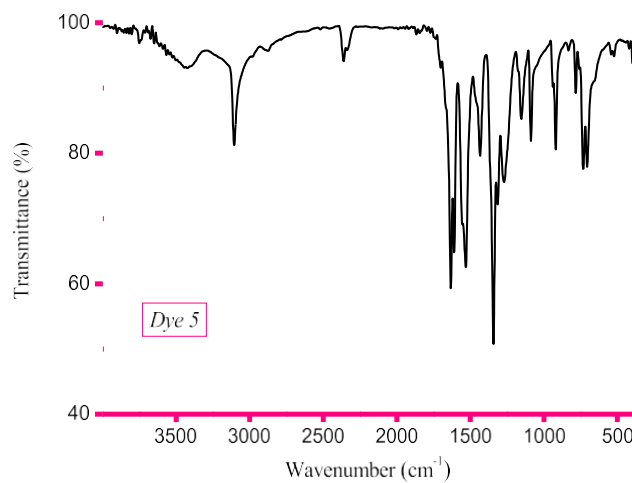


Fig. 11. IR spectra of the free Dye 5 and its CT complex with PA acceptor.

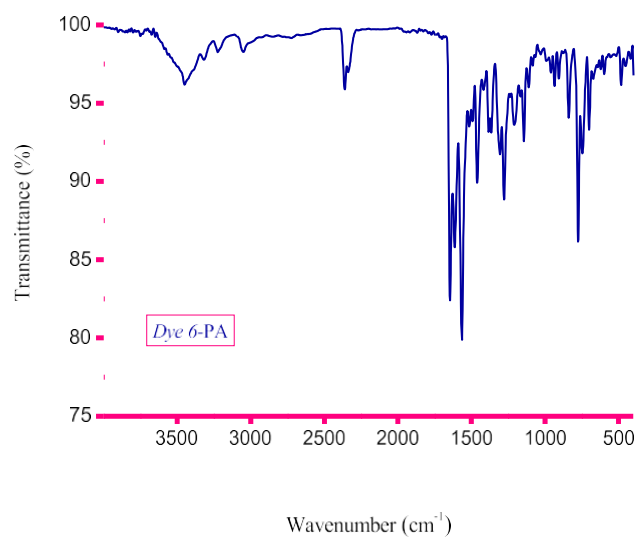
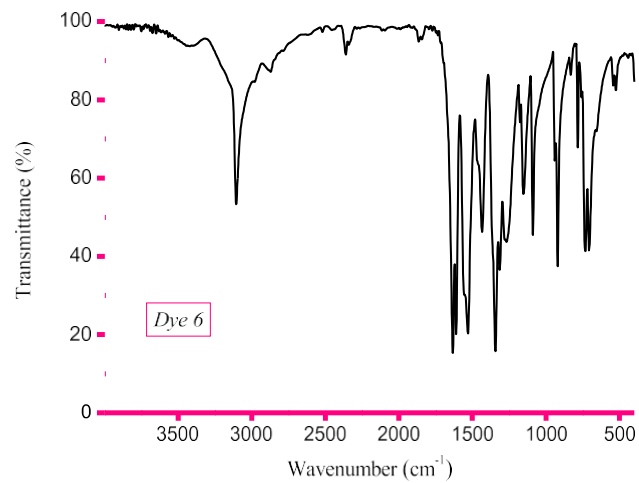


Fig. 12. IR spectra of the free Dye 6 and its CT complex with PA acceptor.

Table 4

IR spectral assignments of the 1,8-naphthalimide dyes (Dye 1-Dye 5) and their CT complexes with PA acceptor.

Free PA	Free dyes					Complexed dyes					Assignments ^a
	Dye 1	Dye 2	Dye 3	Dye 4	Dye 5	Dye 1	Dye 2	Dye 3	Dye 4	Dye 5	
3416	3428	3430	3419	3468	3422	—	—	—	—	3425	$\nu(\text{O} \diagup \text{H})$; H_2O ;
—	—	—	—	—	—	3335	3325	3325	3335	—	$\nu(\text{PA} \diagup \text{H})$
—	—	—	—	3207	3130	—	—	—	—	—	$\nu(\text{N} \diagup \text{H})$
3103	3102	3108	3107	3075	3090	3075	3074	3081	3065	3113	$\nu_{\text{as}}(\text{C} \diagup \text{H})$; aromatic
2980	2959	2961	2957	2975	298	2957	2960	2950	2954	2929	$\nu_{\text{as}}(\text{C} \diagup \text{H}) +$

					0					42	$\nu_s(\text{C}\backslash\text{H})$
—	2872	2873	2866	2815	28 79	2869	2869	2860	2834	28	$\nu_{as}(\text{C}\backslash\text{H}) +$
—	2363	2365	2364	2355	23 65	2358	2357	2358	—	52 23 49	$\nu_s(\text{C}\backslash\text{H})$ Combination band
—	1709	1701	1705	1709	17 02	1706	1704	1710	1709	17 06	$\nu_{as}(\text{C}_\text{O})$
—	1660	1652	1634	1659	16 41	1648	1653	1660	1658	16 66	$\nu_s(\text{C}_\text{O})$
—	—	—	—	1598	16 03	—	—	—	1627	16 24	$\delta(\text{N}\backslash\text{H})$
1632	1533	1536	1534	1540	15 41	1589	1583	1599	1588	15 85	$\nu(\text{C}_\text{C})$ (in-ring), aromatic
1608	—	—	—	—	— —	1501	1502	1519	1517	15 25	$\nu_{as}(\text{NO}_2)$; PA
1529, 1432 1435	1466	1444	1440	1440	14 40	1462	1462	1458	1437	14 45	$\delta(\text{CH})$ deformation
1343	—	—	—	—	— —	1496	1480	1398	1387	13 84	$\nu_s(\text{NO}_2)$; PA
—	1347	1349	1353	1340	13 50	1355	1352	1358	1337	13 54	$\delta(\text{CH})$ deformation
—	1259	1261	1263	—	— —	1267	1261	1267	—	—	$\nu(\text{C}\backslash\text{O})$
—	1250	1262	1247	1269	12 50	1228	1231	1237	1236	12 33	$\delta(\text{C}\backslash\text{C})$
—	1152	1155	1152	1159	11 49	1110	111 1	1137	1136	11 13	$\nu_{as}(\text{C}\backslash\text{N})$
—	1093	1096	1092	1088	10 89	1071	1070	1067	1065	10 68	$\nu_s(\text{C}\backslash\text{N})$
1150, 1086 917	949	920	907	907	91 8	944	940	905	941	87 2	$\delta(\text{CH})$ in-plane bending
781	—	—	—	—	— —	856	849	845	854	84 1	$\delta(\text{NO}_2)$, scissoring; PA
—	790	783	790	787	78 7	788	789	785	786	78 1	$\delta_{rock}(\text{CH})$
—	732	753	730	707	72 7	749	749	744	774	76 1	$\delta(\text{CH})$ out-of- plane bending
703	—	—	—	—	— —	660	658	654	663	65 8	$\omega(\text{NO}_2)$; PA
522	—	—	—	—	— —	573	568	584	577	580	$\delta_{rock}(\text{NO}_2)$; PA

^a ν, stretching; ν_s, symmetrical stretching; ν_{as}, asymmetrical stretching; δ, bending.

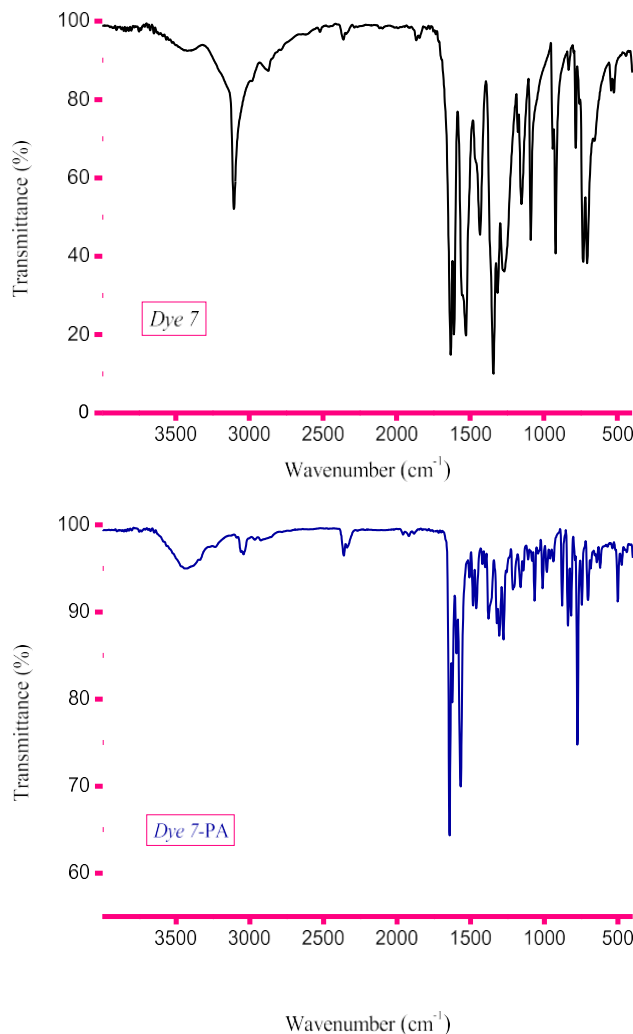


Fig. 13. IR spectra of the free Dye 7 and its CT complex with PA acceptor.

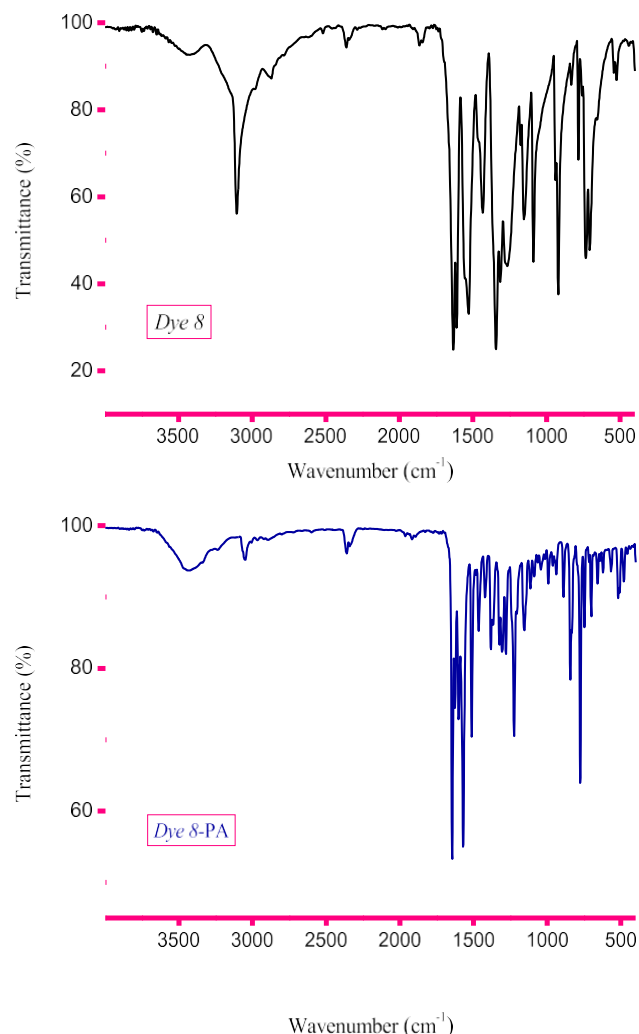


Fig. 14. IR spectra of the free Dye 8 and its CT complex with PA acceptor.

3.3.7. Calculation of R_N

The R_N value was calculated based on the equation theoretically derived by Briegleb and Czekalla [82]:

$$\epsilon_{\max} / 4 \cdot 7:7 \times 10^{-4} = h\nu_{CT} = R_N - 3:5$$

Fig. 3 shows representative 1:1 Benesi–Hildebrand plot of the synthesized CT complexes in methanol solvent. The values of the spectroscopic parameters are listed in Table 3. Generally, the synthesized CT complexes show high values of K_{CT} . The values of K_{CT} for the obtained CT complexes are in the range 1.26×10^6 – $4 \times 10^6 \text{ mol}^{-1}$. The CT complex obtained with Dye 7 exhibits the highest K_{CT} value compared with

other complexes. (Fig. 4). This high value of K_{CT} suggests a high stability of the complex containing Dye 7 in methanol. The stability of the synthesized CT complexes for the different dyes decreases in the following order: Dye 7 N Dye 8 N Dye 6 N Dye 5 N Dye 3 N Dye 4 N Dye 1; Dye 2 N Dye 9. The complex obtained with Dye 6 exhibits higher ϵ_{\max} value compared with other CT complexes. All the ΔG° values are negative, suggesting that the interaction between the PA acceptor and all dyes is spontaneous, and reasonably stable [83]. The ΔG° values of the CT complexes for the different dyes are ordered as follows: Dye 7 N Dye 8 N Dye 6 N Dye 5 N Dye 3 N Dye 4 N Dye 2 N Dye 1 N Dye 9. This ordering is consistent with the stability of the CT complexes. A strong linear correlation ($r = 0.96302$) is observed between ΔG° and K_{CT} values (Fig. 5). The values of

ΔG° become more negative with increasing K_{CT} for the CT complex.

3.4. Band gap energy

The band gap energy (E_g) can be determined from the variation of the optical absorption near the fundamental absorption edge. To E_g , first the absorption coefficient (α) is calculated from the measured ab-sorbance (A) using the relation:

$$\alpha \propto 1/d \ln A$$

δ99

where d is the width of the cell.

Then E_g is calculated using the relation [84–86]:

$$\delta \alpha h v \propto A^{\frac{1}{m}} h v - E_g^{\frac{1}{m}}$$

δ100

where $h v$ is the photon energy, A is an energy independent constant, and m is equal to 2 and $\frac{1}{2}$ for indirect and direct transitions, respectively. The E_g can be evaluated graphically by extrapolating the linear portion of the $(\alpha h v)^{\frac{1}{m}}$ against $h v$ curve to $(\alpha h v)^{\frac{1}{m}} = 0$ [87].

Curves of $(\alpha h v)^{\frac{1}{m}}$ against $h v$ for the PA acceptor, free dyes, and the synthesized CT complexes are given in Fig. 6. The value of E_g for the PA acceptor is 2.57 eV. The values of E_g for free dyes are equal to 2.94, 3.25, 2.96, 3.33, 2.29, 2.39, 2.38, 2.36, 1.69 eV, for Dye 1, Dye 2, Dye 3, Dye 4, Dye 5, Dye 6, Dye 7, Dye 8, and Dye 9, respectively. When these dyes complexed with PA acceptor, the corresponding values for the obtained CT complexes are equal to 2.59, 2.60, 2.60, 2.90, 2.59, 2.57, 2.54, 2.59, and 2.56 eV, respectively. These data indicate that the complexation with PA decreases the band gap energy of the Dye 1, Dye 2, Dye 3, and Dye 4. On the other hand, the complexation with PA increases the

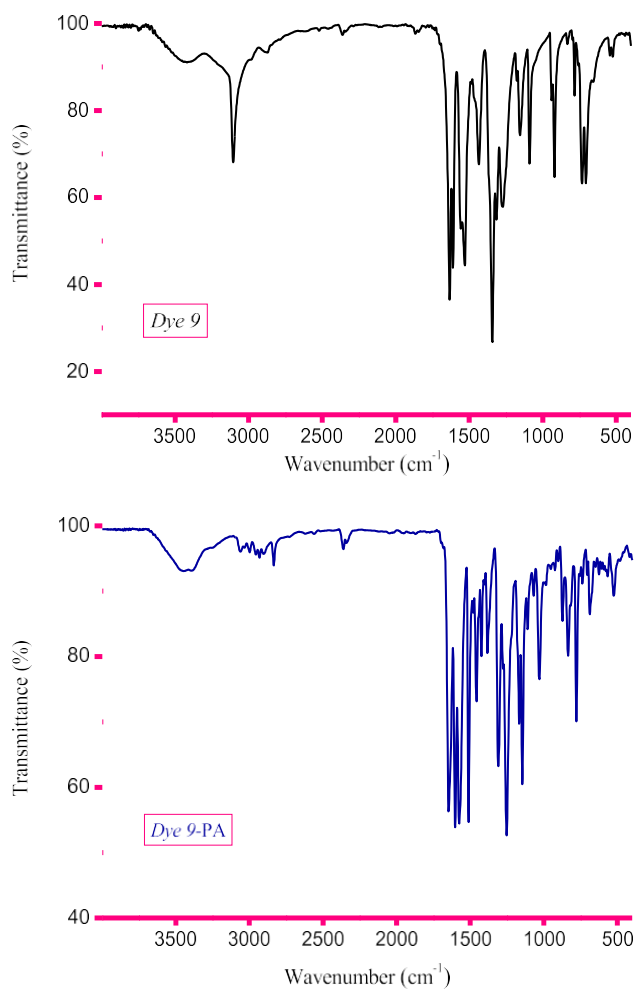


Fig. 15. IR spectra of the free Dye 9 and its CT complex with PA acceptor.

band gap energy of the *Dye 5*, *Dye 6*, *Dye 7*, *Dye 8* and *Dye 9*; the increase in the band gap energy of these dyes are 0.3, 0.18, 0.16, 0.23, and 0.87 eV, respectively.

Generally, the band gap energy of the 1,8-naphthalimide dyes decreases when these dyes complexed with PA acceptor, while the bad gap energy of the benzanthrone dyes increases when these dyes complexed with PA acceptor. We can explain this observation based on two facts: i) the relationship between the band gap energy and the aromaticity is a reversible relation [88], and ii) significant mixing of the *N*- lone pairs of the heterocycle with carbon *p*-orbitals improves the aromaticity and decreases the HOMO–LUMO energy gap [89]. The complexation with PA increases the band gap energy of the benzanthrone dyes because the formation of the positive nitrogen led to the attraction of the π -electrons of the naphthalene ring (the main nucleus of aromaticity of these dyes) and thus decreasing the aromaticity of the complex, and in return, it causes an increase in the band gap energy. On the other hand, the formation of the positive nitrogen in the complexes of 1,8-naphthalimide dyes doesn't affect on the aromaticity of the complex because the positive nitrogen is isolated from the naphthalene ring with a nonaromatic five-membered ring.

3.5. IR spectroscopy

3.5.1. CT complexes with 1,8-naphthalimide derivatives

The IR spectra bands of the free 1,8-naphthalimide derivatives (*Dyes 1–5*) and their CT complexes with the PA acceptor are shown in Figs. 7–11, whereas the peak assignments for the important peaks are reported in Table 4. The IR spectrum of the free PA acceptor shows the following characteristic vibrations: (i) a very strong broad band of $\nu(\text{O}\text{---H})$ at 3416 cm^{-1} ; (ii) bands at 1608 and 1343 cm^{-1} were assigned to $\nu_{\text{as}}(\text{NO}_2)$ and $\nu_s(\text{NO}_2)$ vibrations, respectively; (iii) bending deformation vibrations of $\delta(\text{C}\text{---H})$ appearing at 1529 – 1432 cm^{-1} ; (iv) deformation vibrations of the NO_2 group; and scissoring, wagging, and rocking appearing at 781 , 703 , and 522 cm^{-1} , respectively. The free 1,8-naphthalimide derivatives (*Dyes 1–5*) show the following characteristic vibrations on their IR spectra: (i) $\text{C}\text{---H}$ vibrations: the bands observed in the range of 3100 – 2800 cm^{-1} were assigned to the $\nu_{\text{as}}(\text{C}\text{---H})$ and $\nu_s(\text{C}\text{---H})$. The bands observed at 1460 – 1440 and 1350 – 1340 cm^{-1}

can be attributed to the $\text{C}\diagdown\text{H}$ bending deformation vibrations. The sharp strong band at

$\sim 790 \text{ cm}^{-1}$ was assigned to $\delta_{\text{rock}}(\text{C}\diagdown\text{H})$ vibrations;

Table 5

IR spectral assignments of the benzanthrone dyes (*Dye 6–Dye 9*) and their CT complexes with PA acceptor.

Free PA	Free dyes				Complexed dyes				Assignments ^a
	Dye 6	Dye 7	Dye 8	Dye 9	Dye 6	Dye 7	Dye 8	Dye 9	
3416	3423	3422	3438	3425	3458	3428	3434	3425	$\nu(\text{O}\diagdown\text{H})$; H_2O ; $\nu(\text{N}\diagdown\text{H}\cdots\text{O})$
—	—	—	—	—	3227	3237	3234	3225	
3103	3102	3100	3106	3104	3056	3046	3053	3064	$\nu_{\text{as}}(\text{C}\diagdown\text{H})$; aromatic
2980	2981	2989	2985	2983	—	2905	2891	2993	$\nu_{\text{as}}(\text{C}\diagdown\text{H}) +$ $\nu_s(\text{C}\diagdown\text{H})$
—	2870	2879	2875	2872	—	—	—	2832	$\nu_{\text{as}}(\text{C}\diagdown\text{H}) +$ $\nu_s(\text{C}\diagdown\text{H})$
—	2358	2356	2362	2360	2363	2362	2359	2360	Combination band
—	1634	1643	1639	1636	1644	1647	1652	1646	$\nu(\text{C}_\text{O})$
—	1604	1603	1608	1606	1619	1627	1621	1606	C_N
1632	1534	1532	1528	1526	1559	1567	1571	1576	$\nu(\text{C}_\text{C})$ (in-ring), aromatic
1608	—	—	—	—	1490	1486	1511	1506	$\nu_{\text{as}}(\text{NO}_2)$; PA
1529, 1432	1444	1442	1438	1435	1457	1466	1461	1466	$\delta(\text{CH})$ deformation
1343	—	—	—	—	1377	1386	1380	1385	$\nu_s(\text{NO}_2)$; PA
—	1353	1341	1347	1355	1306	1305	1301	1305	$\delta(\text{CH})$ deformation
—	1261	1268	1262	1272	1213	1217	1227	1250	$\delta(\text{C}\diagdown\text{C})$
—	—	—	940	—	—	998	—	—	$\nu(\text{C}\diagdown\text{F})$
1150, 1086	921	924	915	923	945	954	938	1033	$\delta(\text{CH})$ in-plane bending
—	—	830	—	—	—	843	—	—	$\nu(\text{C}\diagdown\text{Br})$
781	—	—	—	—	905	883	897	872	$\delta(\text{NO}_2)$, scissoring; PA
—	790, 740	784, 743	784, 744	782, 732	774, 754	773, 743	777, 749	782, 741	$\delta_{\text{rock}}(\text{CH})$
—	700	703	704	701	703	712	697	691	$\delta(\text{CH})$ out-of- plane bending
703	—	—	—	—	593	622	566	565	$\omega(\text{NO}_2)$; PA
522	—	—	—	—	483	511	516	531	$\delta_{\text{rock}}(\text{NO}_2)$; PA

^a ν , stretching; ν_s , symmetrical stretching; ν_{as} , asymmetrical stretching; δ , bending.

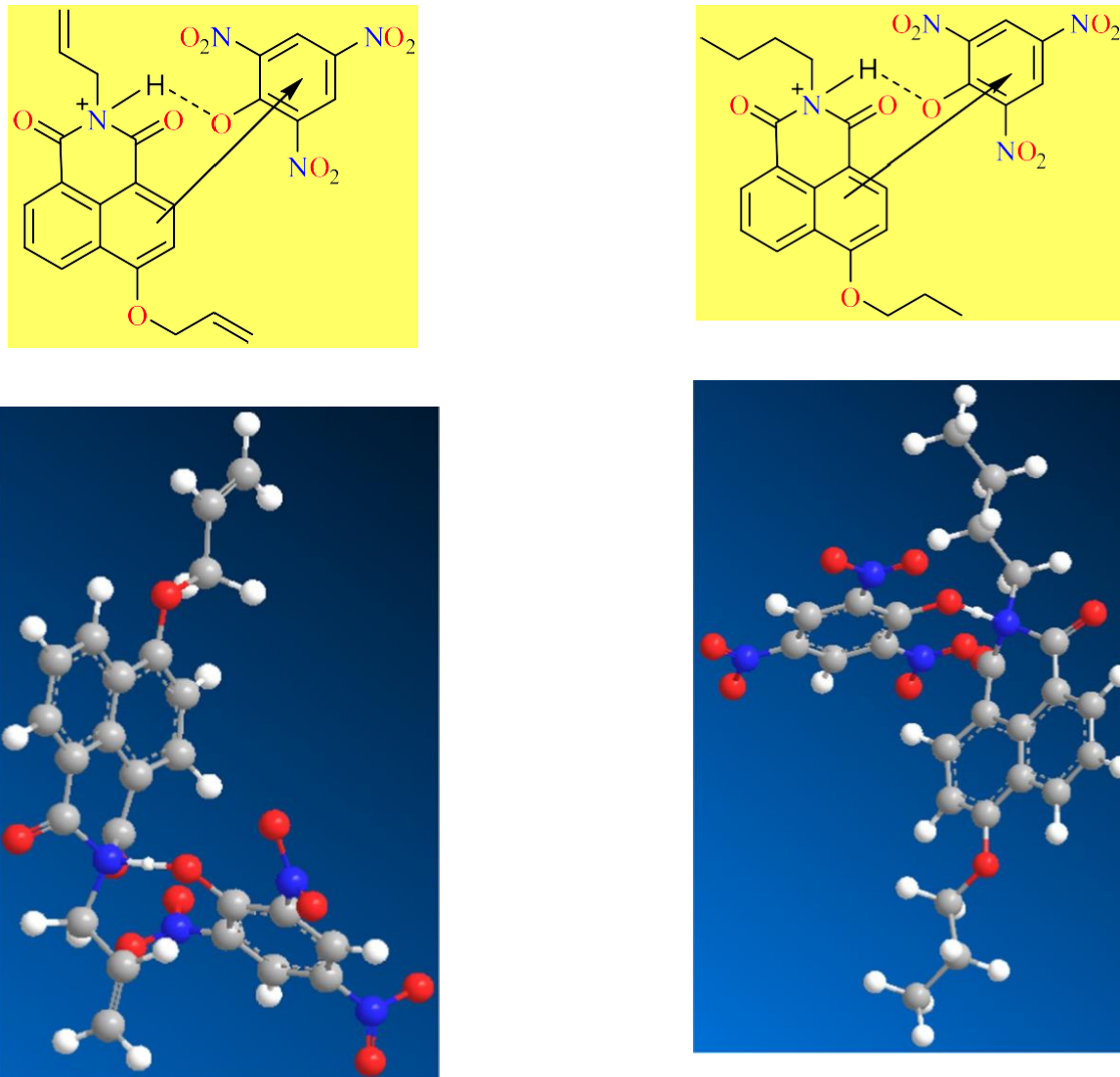


Fig. 16. The proposed structure of the Dye 1—PA complex.

(ii) C_O vibrations: the very strong bands observed at 1710–1700 and 1660–1630 cm^{-1} were assigned to the $\nu_{\text{as}}(\text{C}_\text{O})$ and $\nu_{\text{s}}(\text{C}_\text{O})$ vibrations, respectively; (iii) C_C vibrations: the band observed at approximately 1540–1530 cm^{-1} was assigned to the $\nu(\text{C}_\text{C})$ vibrations; (iv) C_NO vibrations: the band centered at 1270–1260 cm^{-1} was assigned to the $\nu(\text{C}_\text{NO})$ vibrations; (v) C_NN vibrations: bands observed at 1160–1150 cm^{-1} and 1095–1090 cm^{-1} were assigned to C_NN asymmetric and symmetric stretching vibrations, respectively; and (vi) C_CC vibrations: the band centered around 1255 cm^{-1} was assigned to the $\delta(\text{C}_\text{CC})$ vibrations. Also, Dye 4 and Dye 5 exhibit two characteristic vibrations at 3207 and 3130 cm^{-1} that were attributed to the $\nu(\text{N}_\text{NH})$ vibrations, and at 1598 and 1603 cm^{-1}

attributed to the $\delta(\text{N}_\text{NH})$ vibrations, respectively. In the IR spectra of the synthesized

CT complexes, the symmetric and asymmetric C_NH stretching bands appeared in the range 3100–2850 cm^{-1} . The C_O asymmetric stretching vibration band was located around 1710 cm^{-1} , and that of the symmetric stretching vibration around 1660 cm^{-1} . The absorption around 1585 cm^{-1} is due to the aromatic C_C stretching vibrations.

The C_NH deformation mode was observed at the ranges 1460–1440 cm^{-1} and 1355–1350 cm^{-1} . Bands observed at 1135–1110 cm^{-1} and 1070–1065 cm^{-1} were assigned to C_NN asymmetric and symmetric stretching vibrations, respectively. Frequencies of the C_NN band are shifted to lower wavenumbers than that of the free dyes due to the complexation with the PA molecule. The absorption

Fig. 17. The proposed structure of the Dye 2—PA complex.

bands at 1525–1500 cm⁻¹ and at 1398–1380 cm⁻¹ are due to the asym- metric and symmetric stretching vibrations of picrate as for other aromatic nitro groups [90]. Peaks at 855–840, 660–655, and 580–665 cm⁻¹ are due to the scissoring, wagging, and rocking modes of the C≡NNO₂ stretching vibrations, respectively. The nitro vibration

bands, $\nu_{as}(NO_2)$, $\nu_s(NO_2)$, and $\delta(NO_2)$, were shifted with respect to those of the free PA acceptor, likely due to intermolecular CT interactions. The $\nu(O\equiv N-H)$ vibration of the free PA is observed as a strong broad band at 3416 cm⁻¹. This strong broad band was not observed in the spectra of the synthesized CT complexes, suggesting that the OH group of PA was deprotonated towards the dyes' nitrogen atom. A weak band appearing around 3335–3325 cm⁻¹ was observed in the IR spectra of the CT complexes. This band is attributed to the stretching vibration of ($^+N\equiv N-H\cdots O^-$) and confirms the proton transfer from the OH group of the PA acceptor to the nitrogen atom of the dyes to form an intermolecular H-bonded ion pair [91–103]. The three nitro groups in the PA acceptor are electron-withdrawing groups. These groups withdraw electron density from the aromatic ring of PA making it a good electron-accepting molecule. Instead, all the synthesized fluorescent dyes contain high electron densities over the aromatic rings making these dyes good electron-donating molecules. So, the interaction mode between the dyes and the acceptor (Dye → PA) can occur through $\pi \rightarrow \pi^*$ charge migration via the aromatic ring of the dyes and the aromatic ring of the PA acceptor. The $\nu(C-C)$ band of the free dyes ap- peared at 1533, 1536, 1534, 1540, and 1541 cm⁻¹ for Dye 1, Dye 2,

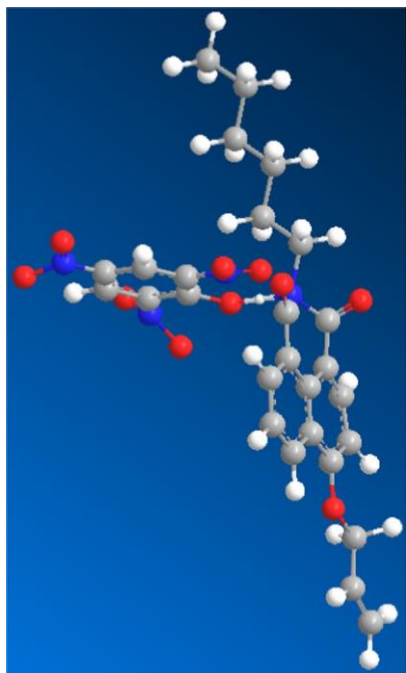
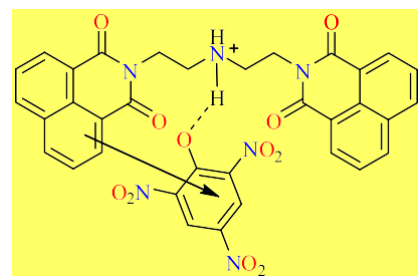


Fig. 18. The proposed structure of the Dye 3-PA complex.

Dye 3, Dye 4, and Dye 5, respectively. Once these dyes interact with the PA acceptor, those bands shift in the corresponding CT complexes to 1589, 1583, 1599, 1588, and 1585 cm^{-1} , respectively. Such shifts suggest that the complexation between those dyes and the PA acceptor can occur through $\pi \rightarrow \pi^*$ interaction along with the proton transfer interaction. The proposed representation of the CT complexes structures is illustrated in Figs. 16–20.

3.5.2. CT complexes with benzanthrone derivatives

The IR spectra bands of the free benzanthrone derivatives (Dyes 6–9) and their CT complexes with the PA acceptor are shown in Figs. 12–15, whereas the peak assignments for the

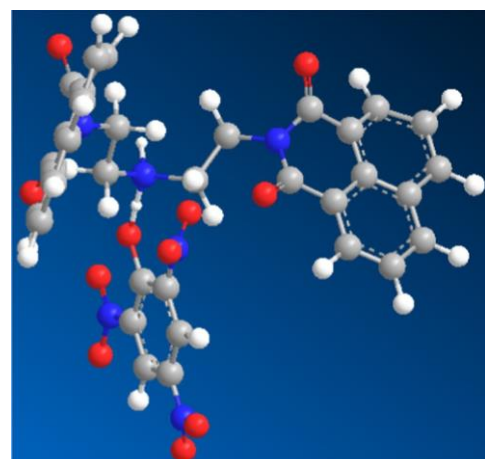
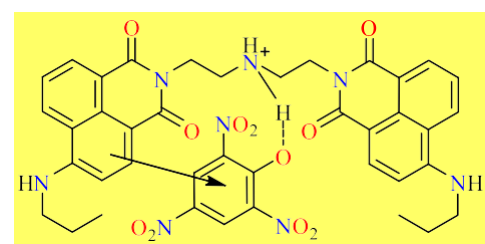


Fig. 19. The proposed structure of the Dye 4-PA complex.

The IR spectra of the free dyes were characterized by a sharp and very strong band around 3100 cm^{-1} due to the $\nu_{as}(\text{C}\equiv\text{N}-\text{H})$ vibrations, but after complexation with the PA acceptor, the intensity of this band significantly decreased. The strong broad band at 3416 cm^{-1} , which is characteristic of $\nu(\text{O}\equiv\text{N}-\text{H})$ vibration of the free PA acceptor, was absent



important peaks are reported in Table 5. Free benzanthrone derivatives (Dyes 6–9) show the following characteristic vibrations in their IR spectra: (i) $\text{C}\equiv\text{N}-\text{H}$ vibrations: the bands observed in the range 3100 – 2850 cm^{-1} were assigned to the $\nu_{as}(\text{C}\equiv\text{N}-\text{H})$ and $\nu_s(\text{C}\equiv\text{N}-\text{H})$.

The bands located around 1440 and 1350 cm^{-1} can be attributed to the C–H bending deformation vibrations. The strong bands at ~784 and ~740 cm^{-1} were assigned to δ_{rock} ($\text{C}\backslash\text{N}\text{H}$) vibrations; (ii) C–O vibrations: the very strong bands observed at 1640–1635 cm^{-1} were assigned to the $\nu(\text{C}_\text{=O})$ vibrations; (iii) C–N vibrations: the bands located around 1605 cm^{-1} were assigned to the $\nu(\text{C}_\text{=N})$ vibrations; (iv) C–C vibrations: the band observed at approximately 1530–1525 cm^{-1} was assigned to the $\nu(\text{C}_\text{–C})$ vibrations; and (v) C–C vibrations: the band centered around 1265 cm^{-1} was assigned to the $\delta(\text{C}\backslash\text{N}\text{C})$ vibrations. Also, in Dye 7, the peak centered at 830 cm^{-1} is probably due to the $\nu(\text{C}\backslash\text{N}\text{Br})$ vibrations, whereas in Dye 8, the peak centered at 940 cm^{-1} is probably due to the $\nu(\text{C}\backslash\text{N}\text{F})$ vibrations.

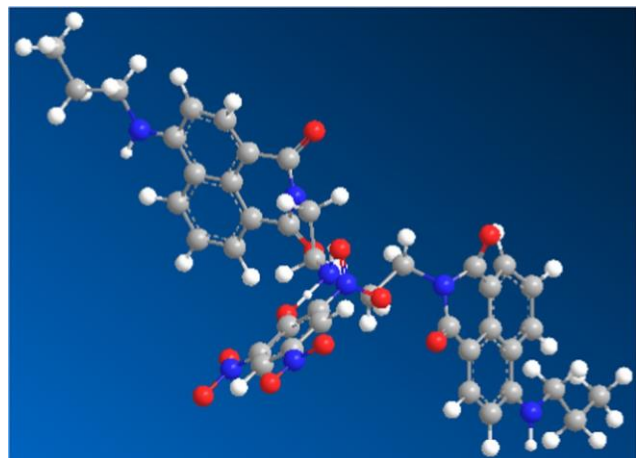


Fig. 20. The proposed structure of the Dye 5—PA complex.

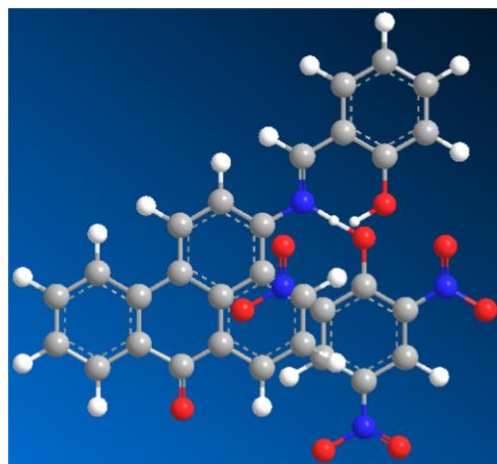
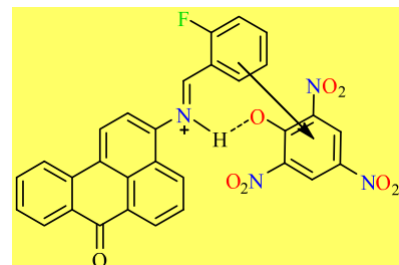
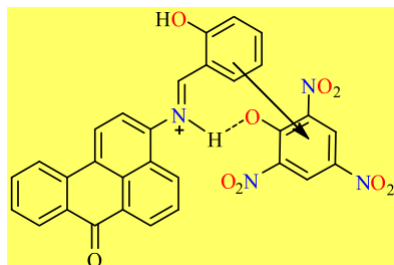


Fig. 21. The proposed structure of the Dye 6—PA complex.

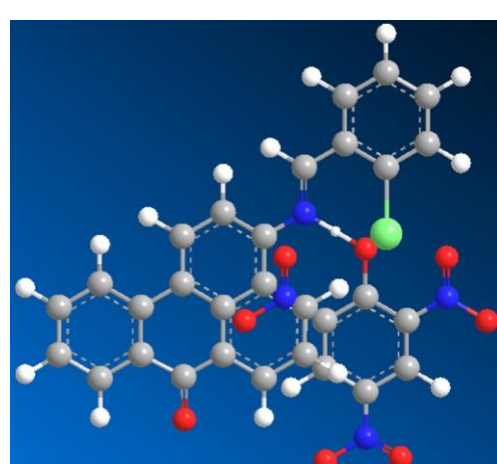


Fig. 23. The proposed structure of the Dye 8—PA complex.

in the spectra of the synthesized CT complexes, suggesting the deprotonation of the OH group of PA towards the nitrogen atom of the dyes. As a result of complexation, the vibrational frequencies of nitro group of the free PA acceptor— $\nu_{as}(NO_2)$, $\nu_s(NO_2)$, $\delta_{sciss.}(NO_2)$, $\omega(NO_2)$, and $\delta_{rock}(NO_2)$ —appearing at 1608, 1343, 781, 703, and 522 cm^{-1} ,

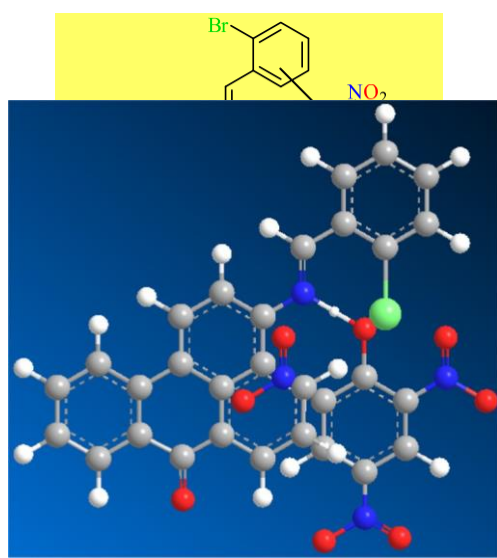
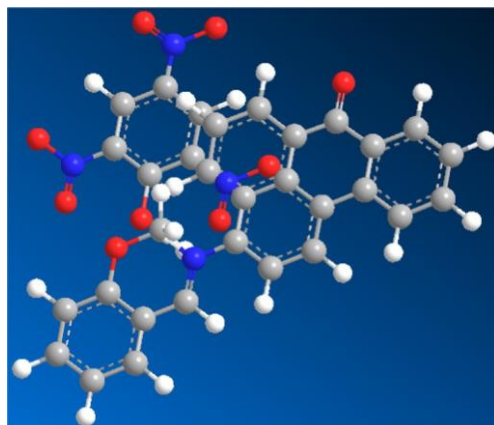
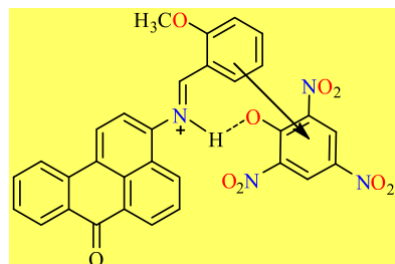


Fig. 22. The proposed structure of the Dye 7—PA complex.

respectively, were shifted and observed in the CT complexes at 1511–1490, 1386–1377, 905–872, 622–565, and 531–483 cm⁻¹, respectively. The new bands observed in the spectra of the synthesized CT complexes at approximately 3237–3225 cm⁻¹ are the result of the stretching vibration of (⁺NH₂H...O⁻), and due to the stretching vibration of a proton attached to the nitrogen atom of the dyes. The band of

Fig. 24. The proposed structure of the Dye 9—PA complex.



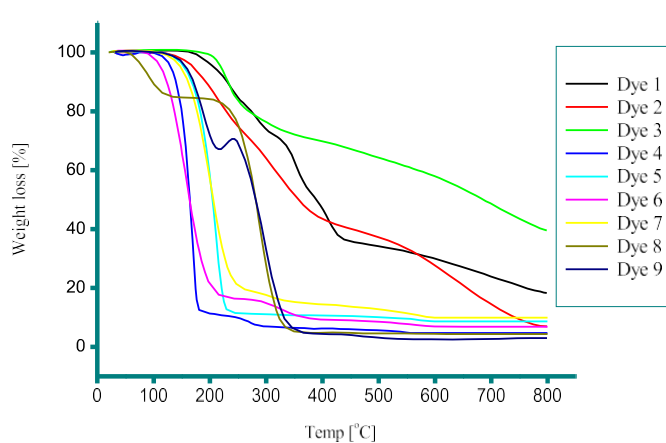


Fig. 25. TGA diagrams of the Dye 1–Dye 9 complexes with PA acceptor.

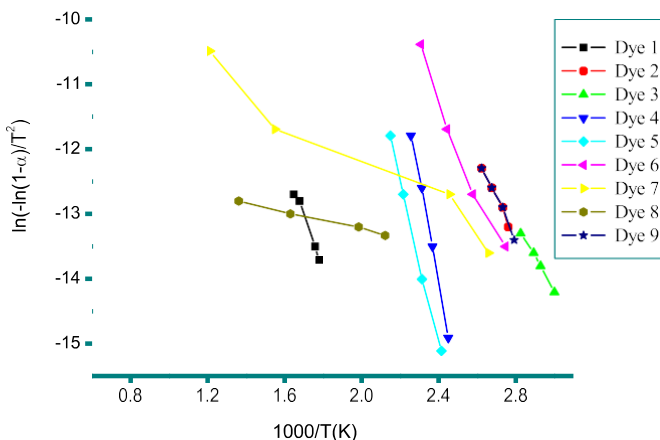


Fig. 26. Coats–Redfern diagrams of the Dye 1–Dye 9 CT complexes with PA acceptor.

$\nu(C-C)$ of the free dyes appeared at 1534, 1532, 1528, and 1526 cm^{-1} for Dye 6, Dye 7, Dye 8, and Dye 9, respectively. Once these dyes interact with the PA acceptor, those bands shift in the corresponding CT complexes to 1559, 1567, 1571, and 1576 cm^{-1} , respectively. All these shifts support the conclusion that a deformation of the electronic environment of the dyes is caused by accepting a proton from the PA molecule and by $\pi \rightarrow \pi^*$ interaction between the dyes and PA molecules, as illustrated in Figs. 21–24.

3.6. Thermal study

TGA curves of the synthesized CT complexes are shown in Fig. 25. The obtained data are supported the thermal stability behaviors of chemical structures proposed for these CT complexes under

investigation. The thermal degradation of the CT complexes proceeds within two-to-three essential degradation steps. The weight losses of Dye 1-PA, Dye 2-PA, Dye 3-PA, Dye 4-PA, Dye 5-PA, Dye 6-PA, Dye 7-PA, Dye 8-PA, and Dye 9-PA complex are 81%, 94%, 61%, 96%, 92%, 93%, 90%, 97%, and 97% corresponding to the decomposition of one of PA and dye molecules. Carbon atoms is the final thermal product remain

as a residue at 800 °C. The kinetic-thermodynamic parameters; the activation energy (E^*), the enthalpy of activation (H^*), the frequency factor (A), the Gibbs free energy of activation (G^*), and the entropy of activation (S^*) were evaluated graphically (Fig. 26) by employing the Coats- Redfern method [104], and the evaluated data are listed in Table 6.

The negative values of (S^*) for the CT complexes indicate that the activated complexes are more ordered than that of either of the reactants.

The reactions for which ΔS^* is negative and ΔG^* is positive are considered as non-spontaneous, so, the thermal degradations of the CT complexes is non-spontaneous, i.e., the synthesized CT complexes are thermally stable.

3. Conclusion

A series of 1,8-naphthalimide and benzanthrone fluorescent dyes were synthesized and characterized. All the synthesized dyes were found to display bright red, orange, or yellow fluorescence in methanol solvent. The ability of the synthesized dyes to react with PA acceptor was evaluated using UV-Vis. and IR spectroscopies. When PA reacted with each dye, a significant change in the UV-Vis. and IR spectra of the formed product was observed compared with those of the free reactants, indicative of

the formation of the CT complex. It has been found that the CT interactions took place via 1:1 molar ratio (Dye: PA). Seven-

eral spectroscopic data (K_{CT} , ϵ_{max} , E_{CT} , f , μ , R_N , I_p , and ΔG°), kinetic- thermodynamic data (E^* , A , ΔS^* , ΔH^* and ΔG^*) and the value of E_g

were estimated for each CT product in methanol solvent at room temperature. The IR data suggest that the complexation between PA and each dye occurs via $\pi \rightarrow \pi^*$ and proton transfer interactions.

Acknowledgement

This work was supported by grants from Vice President for Graduate Study and Research, Taif University, Saudi Arabia under project Grants No. 6011-438-1.

References

- [1] I. Grabchev, V. Bojinov, J. Photochem. Photobiol. A Chem. 139 (2001) 157–160.
- [2] R. Anliker, G. Muller (Eds.), *Fluorescence Whitening Agents in Environmental Quality and Safety*, Vol. 4, Thieme, Stuttgart, 1975.
- [3] M.S. Refat, S.M. Aqeel, I. Grabchev, Can. J. Anal. Sci. Spectrosc. 49 (4) (2004) 258–265.
- [4] O. Zhytniakivska, V. Trusova, G. Gorbenko, E. Kirilova, I. Kalnina, G. Kirilov, P. Kinnunen, J. Lumin. 146 (2014) 307–313.
- [5] T.Z. Philipova, J. Prakt. Chem. 336 (1994) 587–590.
- [6] I. Grabchev, J.M. Chovelon, X. Qian, J. Photochem. Photobiol. A Chem. 158 (2003) 37–43.
- [7] P. Hrdlovič, Š. Chmela, M. Danko, M. Sarakha, G. Guyot, J. Fluoresc. 18 (2008) 393–402.

Table 6

The kinetic-thermodynamic parameters for the synthesized CT complexes using the Coats-Redfern method.

Complexes	Stage	Parameter					r
		E (J mol $^{-1}$)	A (s $^{-1}$)	ΔS (J mol $^{-1}$ /K)	ΔH (J mol $^{-1}$)	ΔG (J mol $^{-1}$)	
Dye 1-PA	1st	0.98×10^9	3.30×10^4	-12.6×10	0.93×10^9	1.62×10^9	0.99 ⁰²
Dye 2-PA	1st	2.30×10^9	9.76×10^{10}	-19.1×10	2.24×10^9	2.90×10^9	0.99 ³²
Dye 3-PA	1st	1.14×10^9	6.54×10^9	-34.8×10	1.10×10^9	2.38×10^9	0.98 ⁹⁰
Dye 4-PA	1st	1.05×10^9	1.23×10^{10}	-8.90×10	0.36×10^9	0.41×10^9	0.99 ⁸⁵
Dye 5-PA	1st	1.22×10^9	5.21×10^9	-12.2×10	0.30×10^9	0.40×10^9	0.99 ²⁰
Dye 6-PA	1st	0.61×10^9	1.54×10^9	-19.4×10	0.34×10^9	0.80×10^9	0.98 ⁶¹

Dye 7-PA	1st	$0.66 \times 10^{-\text{--}}$	$9.21 \times 10^{-\text{--}}$	$-15.1 \times 10^{-\text{--}}$	$0.48 \times 10^{-\text{--}}$	$0.71 \times 10^{-\text{--}}$	$0.99 \times 10^{-\text{--}}$
Dye 8-PA	1st	$0.71 \times 10^{-\text{--}}$	$4.10 \times 10^{-\text{--}}$	$-2.30 \times 10^{-\text{--}}$	$0.59 \times 10^{-\text{--}}$	$0.50 \times 10^{-\text{--}}$	$0.99 \times 10^{-\text{--}}$
Dye 9-PA	1st	1.00×10^5	4.50×10^8	-0.88×10^0	0.98×10^5	1.36×10^5	0.99×10^{12}

- [8] S. Chatterjee, S. Pramanik, S.U. Hossain, S. Bhattacharya, S. Chandra Bhattacharya, *J. Photochem. Photobiol. A Chem.* 187 (2007) 64–71.
- [9] D. Staneva, P. Bosch, A.M. Asiri, L.A. Taib, I. Grabchev, *Dyes Pigments* 105 (2014) 114–120.
- [10] I. Grabchev, D. Staneva, R. Betcheva, *Curr. Med. Chem.* 29 (2012) 4976–4983.
- [11] Z. Li, Y. Zhou, K. Yin, Z. Yu, Y. Li, J. Ren, *Dyes Pigments* 105 (2014) 7–11. [12] F. Sun, R. Jin, J. *Lumin.* 149 (2014) 125–132.
- [13] E. Tamanini, A. Katewa, L. Sedger, M. Todd, M. Watkinson, *Inorg. Chem.* 48 (2009) 319–324.
- [14] T. Philipova, I. Karamancheva, I. Grabchev, *Dyes Pigments* 28 (1995) 91–99.
- [15] I. Grabchev, *Dyes Pigments* 38 (1998) 219–226.
- [16] F. Carlini, C. Paffoni, G. Boffa, *Dyes Pigments* 3 (1982) 59–69.
- [17] T. Konstantinova, H. Konstantinov, T. Kaneva, A. Spirieva, *Polym. Degrad. Stab.* 62 (1998) 323–326.
- [18] X. Yang, W.-H. Liu, W.-J. Jin, G.-L. Shen, R.-Q. Yu, *Spectrochim. Acta A* 55 (1999) 2719–2727.
- [19] G. Gorbenko, V. Trusova, E. Kirilova, G. Kirilov, I. Kalnina, A. Vasilev, S. Kaloyanova, T. Deligeorgiev, *Chem. Phys. Lett.* 495 (2010) 275–279.
- [20] V. Trusova, E. Kirilova, I. Kalnina, G. Kirilov, O. Zhytniakivska, P. Fedorov, G. Gorbenko, *J. Fluoresc.* 22 (2012) 953–959.
- [21] R.S. Mulliken, *J. Phys. Chem.* 56 (1952) 801–805.
- [22] T. Roy, K. Dutta, M.K. Nayek, A.K. Mukherjee, M. Banerjee, B.K. Seal, *J. Chem. Soc. Perkin Trans. 2* (1999) 2219–2223.
- [23] D.K. Roy, A. Saha, A.K. Mukherjee, *Spectrochim. Acta A* 61 (2005) 2017–2022.
- [24] R.K. Gupta, R.A. Sing, *J. Appl. Sci.* 5 (1) (2005) 28–35.
- [25] H.A. Hashem, M.S. Refat, *Surf. Rev. Lett.* 13 (2006) 439–449. [26] A. Tracz, *Pol. J. Chem.* 76 (2002) 457–470.
- [27] U.W. Rabie, M.H. Abou-El-Wafa, R.A. Mohamed, *J. Mol. Struct.* 871 (2007) 6–13.
- [28] M. Kidwai, S. Saxena, S. Rastogi, R. Venkataramanan, *Curr. Med. Chem.: Anti-Infect. Agents* 2 (2004) 269–286.
- [29] F. Gutmann, C. Johnson, H. Keyzer, J. Molnar, *Charge Transfer Complexes in Biochemistry Systems*, Marcel Dekker Inc., 1992
- [30] A. Dozal, H. Keyzer, H.K. Kim, W.W. Way, *Int. J. Antimicrob. Agents* 14 (2000) 261–265.
- [31] S. Seridi, K. Dinar, A. Seridi, M. Berredjem, M. Kadri, *New J. Chem.* 40 (2016) 4781–4792.
- [32] M.E. Mohamed, E.Y.Z. Frag, A.A. Hathoot, E.A. Shalaby, *Spectrochim. Acta A* 189 (2018) 357–365.
- [33] Y. Wu, S. Luo, L. Cao, K. Jiang, L. Wang, J. Xie, Z. Wang, *Anal. Chim. Acta* 976 (2017) 74–83.
- [34] A. Karmakar, B. Singh, *Spectrochim. Acta A* 179 (2017) 110–119.
- [35] M.S. Refat, A.M.A. Adam, M.Y. El-Sayed, *Arab. J. Chem.* 10 (2017) S3482–S3492.
- [36] A. Karmakar, B. Singh, *J. Mol. Liq.* 236 (2017) 135–143.
- [37] R. Mutneja, R. Singh, V. Kaur, J. Wagler, E. Kroke, S.K. Kansal, *Dyes Pigments* 139 (2017) 635–643.
- [38] X. Tian, X. Qi, X. Liu, Q. Zhang, *Sensors Actuators B Chem.* 229 (2016) 520–527.
- [39] T.S. Belal, D.S. El-Kafrawy, M.S. Mahrous, M.M. Abdel-Khalek, A.H. Abo-Gharam, *Spectrochim. Acta A* 155 (2016) 47–53.
- [40] K. Duraimurugan, R. Balasarayanan, A. Siva, *Sensors Actuators B Chem.* 231 (2016) 302–312.
- [41] A.M.A. Adam, M.S. Refat, H.A. Saad, M.S. Hegab, *J. Mol. Liq.* 216 (2016) 192–208.
- [42] S.A.M. Abdulrahman, O.Z. Devi, K. Basavaiah, K.B. Vinay, *J. Taibah Univ. Sci.* 10 (2016) 80–91.
- [43] M.S. Refat, L.A. Ismail, A.M.A. Adam, *Spectrochim. Acta A* 134 (2015) 288–301.
- [44] M.Y. El-Sayed, M.S. Refat, *Spectrochim. Acta A* 137 (2015) 1270–1279.
- [45] M.S. Refat, H.A. Saad, A.M.A. Adam, *Spectrochim. Acta A* 141 (2015) 202–210.
- [46] A.S. Gaballa, A.S. Amin, *Spectrochim. Acta A* 145 (2015) 302–312.
- [47] A.M.A. Adam, M.S. Refat, H.A. Saad, *C.R. Chimie* 18 (2015) 914–928.
- [48] M.S. Refat, A.M.A. Adam, H.A. Saad, *J. Mol. Struct.* 1085 (2015) 178–190.
- [49] A. Gupta, Y. Kang, M. Choi, J.S. Park, *Sensors Actuators B Chem.* 209 (2015) 225–229.
- [50] I.M. Al-Harbi, E.H. El-Mossallamy, A.Y. Obaid, A.H. Al-Jedaani, *Spectrochim. Acta A* 120 (2014) 25–31.
- [51] H.H. Eldaroti, S.A. Gadir, M.S. Refat, A.M.A. Adam, *J. Pharm. Anal.* 4 (2) (2014) 81–95.
- [52] M.S. Refat, S.M. Teleb, I. Grabchev, *Spectrochim. Acta A* 61 (1-2) (2005) 205–211.
- [53] A.M.A. Adam, *Spectrochim. Acta A* 104 (2013) 1–13.
- [54]

- G. Bator, L. Sobczyk, W. Sawka-Dobrowolska, J. Wuttke, A. Pawlukojc, E. Grech, J. Nowicka-Scheibe, *Chem. Phys.* 410 (2013) 55–65.
- [55] A.M.A. Adam, M.S. Refat, H.A. Saad, *J. Mol. Struct.* 1037 (2013) 376–392.
- [56] A.M.A. Adam, *J. Mol. Struct.* 1030 (2012) 26–39.
- [57] I.M. Khan, A. Ahmad, M.F. Ullah, *J. Photochem. Photobiol. B* 103 (2011) 42–49.
- [58] M.S. Refat, H.A. Saad, A.M.A. Adam, *Spectrochim. Acta A* 79 (2011) 672–679.
- [59] N. Singh, I.M. Khan, A. Ahmad, *Spectrochim. Acta A* 75 (2010) 1347–1353.
- [60] I.M. Khan, A. Ahmad, *Spectrochim. Acta A* 77 (2010) 437–441.
- [61] I.M. Khan, A. Ahmad, M. Oves, *Spectrochim. Acta A* 77 (2010) 1059–1064.
- [62] N. Singh, A. Ahmad, *J. Mol. Struct.* 977 (2010) 197–202.
- [63] I. Grabchev, T. Konstantinova, *Dyes Pigments* 33 (1997) 197–203.
- [64] R. S-C Chang, D. Lewis Utecht, *Dyes Pigments* 43 (1999) 83–94.
- [65] I. Grabchev, C. Petkov, V. Bojinov, *Dyes Pigments* 48 (2001) 239–244.
- [66] V. Bojinov, I. Grabchev, *Dyes Pigments* 51 (2001) 57–61.
- [67] I. Grabchev, I. Moneva, V. Bojinov, S. Guittonneau, *J. Mater. Chem.* 10 (2000) 1291–1296.
- [68] I. Grabchev, R. Betcheva, *J. Photochem. Photobiol. A Chem.* 142 (2001) 73–78.
- [69] I. Grabchev, I. Moneva, C.R. Acad., Bulg. Sci. 50 (6) (1997) 59–62.
- [70] I. Grabchev, I. Moneva, *Dyes Pigments* 37 (1998) 155–165.
- [71] I. Grabchev, V. Bojinov, I. Moneva, *J. Mol. Struct.* 471 (1998) 19–25.
- [72] M. Salman, M.S. Refat, I. Grabchev, A.M.A. Adam, *Int. J. Electrochem. Sci.* 8 (2) (2013) 2863–2879.
- [73] A.S.A. Almalki, A.M. Naglah, M.S. Refat, M.S. Hegab, A.M.A. Adam, M.A. Al-Omar, *J. Mol. Liq.* 233 (2017) 292–302.
- [74] A.M.A. Adam, M.S. Refat, *J. Mol. Liq.* 219 (2016) 377–389.
- [75] A.M.A. Adam, M.S. Refat, M.S. Hegab, H.A. Saad, *J. Mol. Liq.* 224 (2016) 311–321.
- [76] H.A. Benesi, J.H. Hildebrand, *J. Am. Chem. Soc.* 71 (1949) 2703–2707.
- [77] G. Briegleb, *Z. Angew. Chem.* 76 (1964) 326–341.
- [78] A.N. Martin, J. Swarbrick, A. Cammarata, *Physical Pharmacy*, 3rd ed. Lee and Febiger, Philadelphia, PA, 1969 344.
- [79] R. Rathore, S.V. Lindeman, J.K. Kochi, *J. Am. Chem. Soc.* 119 (1997) 9393–9404.
- [80] H. Tsubomura, R.P. Lang, *J. Am. Chem. Soc.* 83 (1961) 2085–2092.
- [81] G.G. Aloisi, Pignataro, *J. Chem. Soc. Faraday Trans.* 69 (1973) 534–539.
- [82] G. Briegleb, J. Czekalla, *Z. Physikchem. Z. Phys. Chem. (Frankfurt)* 24 (1960) 237.
- [83] M. Pandeeswaran, K.P. Elango, *Spectrochim. Acta A* 65 (2006) 1148–1153.
- [84] N.F. Mott, E.A. Davis, *Electrochemical Process in Non-crystalline Materials*, Calendron Press, Oxford, 1979.
- [85] F. Karipcin, B. Dede, Y. Caglar, D. Hur, S. Ilican, M. Caglar, Y. Sahin, *Opt. Commun.* 272 (2007) 131–137.
- [86] F. Yakuphanoglu, A. Cukurovali, I. Yilmaz, *Opt. Mater.* 27 (2005) 1363–1368.
- [87] M. Hoffman, S. Martin, W. Choi, D. Bahnemann, *Chem. Rev.* 95 (1995) 69–96.
- [88] S. Gümüş, L. Türker, *Heterocycl. Commun.* 18 (1) (2012) 11–16, <https://doi.org/10.1515/hc-2011-0050>.
- [89] R. Rakhi, C.H. Suresh, *Chem. Phys.* 18 (35) (2016) 24631–24641, <https://doi.org/10.1039/c6cp03723b>.
- [90] G.A. Babu, A. Chandramohan, P. Ramasamy, G. Bhagavannarayana, B. Varghese, *Mater. Res. Bull.* 46 (2011) 464–468.
- [91] E. Selyakumar, G.A. Babu, P. Ramasamy, A. Chandramohan, *Spectrochim. Acta A* 122 (2014) 436–440.
- [92] N. Singh, A. Ahmad, *J. Mol. Struct.* 1074 (2014) 408–415.
- [93] N. Singh, I.M. Khan, A. Ahmad, S. Javed, *J. Mol. Liq.* 191 (2014) 142–150.
- [94] N. Singh, I.M. Kahn, A. Ahmed, S. Javed, *Mol. Struct.* 1065–1066 (2014) 74–85.
- [95] X. Ding, Y. Li, S. Wang, X. Li, W. Huang, *J. Mol. Struct.* 1062 (2014) 61–67.
- [96] M. Manikandan, T. Mahalingam, Y. Hayakawa, G. Ravi, *Spectrochim. Acta A* 101 (2013) 178–183.
- [97] I.M. Khan, A. Ahmad, *J. Mol. Struct.* 1050 (2013) 122–127.
- [98] I.M. Khan, A. Ahmad, S. Kumar, *J. Mol. Struct.* 1035 (2013) 38–45.
- [99] I.M. Khan, A. Ahmad, M.F. Ullah, *Spectrochim. Acta A* 102 (2013) 82–87.
- [100] X. Ding, Y. Li, S. Wang, X. Li, W. Huang, *J. Mol. Struct.* 1051 (2013) 124–131.
- [101] H.H. Eldaroti, S.A. Gadir, M.S. Refat, A.M.A. Adam, *Spectrochim. Acta A* 115 (2013) 309–323.
- [102] H.H. Eldaroti, S.A. Gadir, M.S. Refat, A.M.A. Adam, *Spectrochim. Acta A* 109 (2013) 259–271.
- [103] R.L. Frost, O.B. Locos, H. Ruan, J.T. Kloprogge, *Vib. Spectrosc.* 27 (2001) 1–3.
- [104] A.W. Coats, J.P. Redfern, *Nature* 201 (1964) 68.